Minimal complete sets for two-pseudoscalar-meson photoproduction

Philipp Kroenert ⬤,* Yannick Wunderlich ⬤, Farah Afzal ⬤, and Annika Thiel ⬤

Helmholtz Institut für Strahlen- und Kernphysik, Universität Bonn, Germany

For photoproduction reactions with final states consisting of two pseudoscalar mesons and a spin-1/2 baryon, eight complex amplitudes need to be determined uniquely. A modified version of Moravcsik's theorem is employed for these reactions, resulting in slightly overcomplete sets of polarization observables that are able to determine the amplitudes uniquely. Further steps were taken to reduce the found sets to minimal complete sets. As a final result, multiple minimal complete sets without any remaining ambiguities are presented for the first time. These sets consist of $2N = 16$ observables, containing only one triple polarization observable.

I. INTRODUCTION

The interrelation between experiment and theory is what drives science. In the field of hadron spectroscopy these are the measurement of cross sections or polarization observables and its counterpart Quantum Chromodynamics. The latter describes the transition of the initial to the final state via a transition matrix $\mathcal{T}$. This matrix comprises the employed model predictions to describe a certain process. Via so-called formation experiments (i.e., $\gamma p \rightarrow \pi \pi p$) it is possible to study the emergence of resonant states [such as $\Delta(1232)$, $N(1440)1/2+$, $N(1520)3/2-$, etc. [1]].

These states can be analyzed via partial-wave analysis (i.e., BnGa [1], MAID [2]), determining the matrix elements of $\mathcal{T}$ and comparing it to the model prediction. However, because polarization observables depend on bilinear products of the complex amplitudes [3–5], mathematical ambiguities arise [6]. Nevertheless, it is still possible to determine unique solutions by employing a complete experiment analysis [7].

Such a complete experiment analysis was performed analytically by Chiang and Tabakin in 1997 [6] for single pseudoscalar meson photoproduction. A detailed proof comprising all the relevant cases was published recently by Nakayama [8]. It should be noted that these complete experiments are an idealization for data with no uncertainty [9]. Although the process of single pseudoscalar meson photoproduction can be fully described by only four complex amplitudes [10], the calculations are nontrivial and cumbersome [8] and, furthermore, quite involved ambiguity-structures can arise.

Within this paper, the determination of complete sets of observables is studied for the reaction of two pseudoscalar meson photoproduction. The process can be described by $N = 8$ complex amplitudes and thus allows for 64 measurable polarization observables [5], which are four times as many observables as in the case of single pseudoscalar

meson photoproduction [6]. This results in an exponential increase of complexity, for what reason the algebraic techniques presented in Ref. [8] are no longer appropriate, although possible (see Sec. VII B). New methods should be employed, in order to allow for an easier access to the problem of complete sets for reactions with $N > 4$.

There is an already existing work on this subject by Arenhövel and Fix [11] from 2014. On the one hand, they used the inverse function theorem to derive complete sets of 16 observables. The downside of this method is that the resulting sets might locally be free of ambiguities, but not globally. On the other hand, they used a graph theoretical approach, where a complex amplitude is represented as a node and the bilinear product as a connection between certain nodes. This method yields complete sets with 25 observables. It was then shown how to further reduce such a set to 15 observables. Although they found sets without triple polarization observables, there still remain quadratic ambiguities.

To overcome these difficulties arising from the remaining discrete mathematical ambiguities, Moravcsik's theorem [12] is employed within this paper. This theorem allows for the extraction of complete sets of observables for an arbitrary number of amplitudes. Furthermore, due to its graph-theoretical foundation, the whole algorithm can be automated [13].

The paper is structured in the following way: The starting point is a short recap of Moravcsik's theorem and its modification in Sec. II. Section III introduces the 64 polarization observables for two pseudoscalar meson photoproduction. Within Sec. IV the actual application of Moravcsik's theorem is described and illustrated with an example. Section V elaborates on the difficulties of the experimental determination of the polarization observables and gives an extensive overview of already-performed measurements in two pseudoscalar meson photoproduction. The entire analysis results in 5964 unique, but slightly overcomplete sets of observables. Their characteristics are discussed in Sec. VI. Section VII describes how to transform the slightly overcomplete sets into minimal ones (i.e., into sets containing $2N = 16$ observables). Based on these sets as well as the already-performed measure-

---

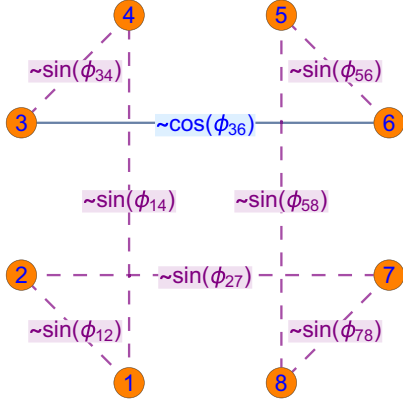*Corresponding author: kroenert@hiskp.uni-bonn.de

FIG. 1. Illustration of a cycle graph with eight nodes (enumerated points) and edges (solid and dashed lines). Each node represents one complex amplitude, whereas each edge connecting two nodes represents either the real (solid) or imaginary (dashed) part of the bilinear product of those nodes. The respective correlation to the relative phase ϕ_{ij} is indicated.

ments the most promising minimal complete set is presented in Sec. VIII. The results are summarized in Sec. IX.

II. MORAVCSIK'S THEOREM

The main points of Moravcsik's paper [12] shall be recapped in a concise form. The basic assumption of the theorem is that the moduli of the N complex amplitudes t_i are known, together with the real and imaginary parts of the bilinear products $t_i t_j^*$. Furthermore, each complex amplitude t_i is treated as a node of a graph whereas an edge is the real or imaginary part of the bilinear amplitude product $t_i t_j^*$ connecting both nodes. An illustration is shown in Fig. 1. Such a graph is said to correspond to a complete set of observables if it fulfills the following two requirements:

(1) it is a connected graph;
(2) it has an odd number of edges which corresponds to an imaginary part of a particular bilinear product, i.e., $\propto \text{Im}(t_i t_j^*)$.

The first condition is related to the "consistency relation" of the relative phases:

$$\phi_{12} + \phi_{23} + \cdots + \phi_{N1} = 0, \qquad (1)$$

which implies a summation of relative phases between all neighboring amplitudes t_i [8]. Equation (1) has to hold in every case, whether the considered set is fully complete or not. The second condition is responsible for resolving the discrete ambiguities since it holds

$$\text{Im}(t_i t_j^*) = |t_i||t_j| \sin(\phi_{ij}), \qquad (2)$$

and that sine itself produces an ambiguity due to its periodicity:

$$\phi_{ij} \rightarrow (\phi_{ij}, \pi - \phi_{ij}). \qquad (3)$$

It turns out that any odd number of such "sine-type" ambiguities resolves the discrete ambiguities, due to the summand π.

The generalization to any odd number is the actual modification to Moravcsik's theorem. A proof of the original version of the theorem can be found in Ref. [12] and a quite detailed proof of the modified version of the theorem is given in Ref. [13].

The following analysis focuses on cycle graphs, i.e., connected graphs where each node has degree two. As explained in Ref. [12], "from the point of view of eliminating discrete ambiguities" these graph types are "the most economical" ones. Thus, only the minimal number of N bilinear products is needed in order to eliminate all discrete ambiguities, one for each edge.

III. POLARIZATION OBSERVABLES

The derivation of the 64 polarization observables of two pseudoscalar meson photoproduction was first published by Roberts and Oed [5]. The observables were defined in a "helicity and hybrid helicity-transversity basis" [5]. For the latter, the photon spin is still quantized along its direction of motion. For the sake of comparability, the hybrid basis shall be adopted in this paper. However, in order to work out the connection between the real (imaginary) part of the bilinear products and the relative phases ϕ_{ij}, it is advantageous to rename the amplitudes:

$$b_1^+ \rightarrow t_1, \quad b_2^+ \rightarrow t_2, \quad b_3^+ \rightarrow t_3, \quad b_4^+ \rightarrow t_4, \qquad (4)$$

$$b_1^- \rightarrow t_5, \quad b_2^- \rightarrow t_6, \quad b_3^- \rightarrow t_7, \quad b_4^- \rightarrow t_8. \qquad (5)$$

Within Ref. [5], the observables are ordered according to the polarization of the photon beam, which is required to measure the respective observable. This ordering scheme is advantageous from an experimental point of view; unfortunately, it is inappropriate when studying ambiguities. Therefore, the observables are regrouped according to their mathematical structure, which yields eight groups. While the first group consists of observables solely described by the squared moduli of the amplitudes t_i, any other group comprises equal amounts of observables containing only cos or sin terms. The resulting expressions for the observables are listed in Table I.

For the purpose of an easier calculation, 64 Γ matrices are introduced, which can be solely described by the identity matrix, as well as the three Pauli matrices (listed in Table II). This allows us to calculate the respective observable by the bilinear form $\langle t|\Gamma|t \rangle$ with $|t\rangle := (t_1, t_2, t_3, t_4, t_5, t_6, t_7, t_8)$, similar as in Ref. [6]. As expected, the Γ matrices for each group share the same matrix structure. Naturally, they form an orthogonal basis and are Hermitian and unitary. Indeed, the matrices fulfill the same properties as presented in Ref. [6] (with an adapted prefactor in the orthogonality relation).

IV. APPROACH

The results of Sec. II imply the following steps: One constructs all unique graph topologies with N nodes using combinatorial methods. A few examples of possible graphs are shown in Fig. 2. The number of unique topologies is solely determined by the number of nodes (or edges), i.e., for $N \geqslant 3$ it is $N!/(2N)$ [13].

TABLE I. Definitions of the 64 polarization observables for two pseudoscalar meson photoproduction in hybrid helicity-transversity form. Here, ϕ_{ij} denotes the relative phase between the complex amplitudes t_i and t_j. The notation used in the original paper of Roberts and Oed [5] is also shown. The observables are classified into eight groups according to their underlying mathematical structure. The vector $|t\rangle$ has the form $(t_1, t_2, t_3, t_4, t_5, t_6, t_7, t_8)$ and the shape of the Γ matrices is outlined in Table II.

Observable	Definition in terms of polar coordinates / 2	Bilinear form	Roberts, Oed
$\mathcal{O}_1^{I}$	$\frac{1}{2}(|t_1|^2 + |t_2|^2 + |t_3|^2 + |t_4|^2 - |t_5|^2 - |t_6|^2 - |t_7|^2 - |t_8|^2)$	$\langle t|\Gamma_1^{I}|t\rangle$	$I^{\odot}$
$\mathcal{O}_2^{I}$	$\frac{1}{2}(|t_1|^2 + |t_2|^2 - |t_3|^2 - |t_4|^2 + |t_5|^2 + |t_6|^2 - |t_7|^2 - |t_8|^2)$	$\langle t|\Gamma_2^{I}|t\rangle$	P_y
$\mathcal{O}_3^{I}$	$\frac{1}{2}(|t_1|^2 - |t_2|^2 + |t_3|^2 - |t_4|^2 + |t_5|^2 - |t_6|^2 + |t_7|^2 - |t_8|^2)$	$\langle t|\Gamma_3^{I}|t\rangle$	$P_{y'}$
$\mathcal{O}_4^{I}$	$\frac{1}{2}(|t_1|^2 - |t_2|^2 - |t_3|^2 + |t_4|^2 - |t_5|^2 + |t_6|^2 + |t_7|^2 - |t_8|^2)$	$\langle t|\Gamma_4^{I}|t\rangle$	$\mathcal{O}_{yy'}^{\odot}$
$\mathcal{O}_5^{I}$	$\frac{1}{2}(|t_1|^2 - |t_2|^2 - |t_3|^2 + |t_4|^2 + |t_5|^2 - |t_6|^2 - |t_7|^2 + |t_8|^2)$	$\langle t|\Gamma_5^{I}|t\rangle$	$\mathcal{O}_{yy'}$
$\mathcal{O}_6^{I}$	$\frac{1}{2}(|t_1|^2 - |t_2|^2 + |t_3|^2 - |t_4|^2 - |t_5|^2 + |t_6|^2 - |t_7|^2 + |t_8|^2)$	$\langle t|\Gamma_6^{I}|t\rangle$	$P_{y'}^{\odot}$
$\mathcal{O}_7^{I}$	$\frac{1}{2}(|t_1|^2 + |t_2|^2 - |t_3|^2 - |t_4|^2 - |t_5|^2 - |t_6|^2 + |t_7|^2 + |t_8|^2)$	$\langle t|\Gamma_7^{I}|t\rangle$	$P_y^{\odot}$
$\mathcal{O}_8^{I}$	$\frac{1}{2}(|t_1|^2 + |t_2|^2 + |t_3|^2 + |t_4|^2 + |t_5|^2 + |t_6|^2 + |t_7|^2 + |t_8|^2)$	$\langle t|\Gamma_8^{I}|t\rangle$	I_0
$\mathcal{O}_{c1}^{II}$	$|t_1||t_3|\cos(\phi_{13}) + |t_2||t_4|\cos(\phi_{24}) + |t_5||t_7|\cos(\phi_{57}) + |t_6||t_8|\cos(\phi_{68})$	$\langle t|\Gamma_{c1}^{II}|t\rangle$	$-P_z$
$\mathcal{O}_{c2}^{II}$	$|t_1||t_3|\cos(\phi_{13}) + |t_2||t_4|\cos(\phi_{24}) - |t_5||t_7|\cos(\phi_{57}) - |t_6||t_8|\cos(\phi_{68})$	$\langle t|\Gamma_{c2}^{II}|t\rangle$	$-P_z^{\odot}$
$\mathcal{O}_{c3}^{II}$	$|t_1||t_3|\cos(\phi_{13}) - |t_2||t_4|\cos(\phi_{24}) + |t_5||t_7|\cos(\phi_{57}) - |t_6||t_8|\cos(\phi_{68})$	$\langle t|\Gamma_{c3}^{II}|t\rangle$	$-\mathcal{O}_{zy'}$
$\mathcal{O}_{c4}^{II}$	$|t_1||t_3|\cos(\phi_{13}) - |t_2||t_4|\cos(\phi_{24}) - |t_5||t_7|\cos(\phi_{57}) + |t_6||t_8|\cos(\phi_{68})$	$\langle t|\Gamma_{c4}^{II}|t\rangle$	$-\mathcal{O}_{zy'}^{\odot}$
$\mathcal{O}_{s1}^{II}$	$|t_1||t_3|\sin(\phi_{13}) + |t_2||t_4|\sin(\phi_{24}) + |t_5||t_7|\sin(\phi_{57}) + |t_6||t_8|\sin(\phi_{68})$	$\langle t|\Gamma_{s1}^{II}|t\rangle$	$-P_x$
$\mathcal{O}_{s2}^{II}$	$|t_1||t_3|\sin(\phi_{13}) + |t_2||t_4|\sin(\phi_{24}) - |t_5||t_7|\sin(\phi_{57}) - |t_6||t_8|\sin(\phi_{68})$	$\langle t|\Gamma_{s2}^{II}|t\rangle$	$-P_x^{\odot}$
$\mathcal{O}_{s3}^{II}$	$|t_1||t_3|\sin(\phi_{13}) - |t_2||t_4|\sin(\phi_{24}) + |t_5||t_7|\sin(\phi_{57}) - |t_6||t_8|\sin(\phi_{68})$	$\langle t|\Gamma_{s3}^{II}|t\rangle$	$-\mathcal{O}_{xy'}$
$\mathcal{O}_{s4}^{II}$	$|t_1||t_3|\sin(\phi_{13}) - |t_2||t_4|\sin(\phi_{24}) - |t_5||t_7|\sin(\phi_{57}) + |t_6||t_8|\sin(\phi_{68})$	$\langle t|\Gamma_{s4}^{II}|t\rangle$	$-\mathcal{O}_{xy'}^{\odot}$
$\mathcal{O}_{c1}^{III}$	$|t_1||t_2|\cos(\phi_{12}) + |t_3||t_4|\cos(\phi_{34}) + |t_5||t_6|\cos(\phi_{56}) + |t_7||t_8|\cos(\phi_{78})$	$\langle t|\Gamma_{c1}^{III}|t\rangle$	$-P_{z'}$
$\mathcal{O}_{c2}^{III}$	$|t_1||t_2|\cos(\phi_{12}) + |t_3||t_4|\cos(\phi_{34}) - |t_5||t_6|\cos(\phi_{56}) - |t_7||t_8|\cos(\phi_{78})$	$\langle t|\Gamma_{c2}^{III}|t\rangle$	$-P_{z'}^{\odot}$
$\mathcal{O}_{c3}^{III}$	$|t_1||t_2|\cos(\phi_{12}) - |t_3||t_4|\cos(\phi_{34}) + |t_5||t_6|\cos(\phi_{56}) - |t_7||t_8|\cos(\phi_{78})$	$\langle t|\Gamma_{c3}^{III}|t\rangle$	$-\mathcal{O}_{yz'}$
$\mathcal{O}_{c4}^{III}$	$|t_1||t_2|\cos(\phi_{12}) - |t_3||t_4|\cos(\phi_{34}) - |t_5||t_6|\cos(\phi_{56}) + |t_7||t_8|\cos(\phi_{78})$	$\langle t|\Gamma_{c4}^{III}|t\rangle$	$-\mathcal{O}_{yz'}^{\odot}$
$\mathcal{O}_{s1}^{III}$	$|t_1||t_2|\sin(\phi_{12}) + |t_3||t_4|\sin(\phi_{34}) + |t_5||t_6|\sin(\phi_{56}) + |t_7||t_8|\sin(\phi_{78})$	$\langle t|\Gamma_{s1}^{III}|t\rangle$	$P_{x'}$
$\mathcal{O}_{s2}^{III}$	$|t_1||t_2|\sin(\phi_{12}) + |t_3||t_4|\sin(\phi_{34}) - |t_5||t_6|\sin(\phi_{56}) - |t_7||t_8|\sin(\phi_{78})$	$\langle t|\Gamma_{s2}^{III}|t\rangle$	$P_{x'}^{\odot}$
$\mathcal{O}_{s3}^{III}$	$|t_1||t_2|\sin(\phi_{12}) - |t_3||t_4|\sin(\phi_{34}) + |t_5||t_6|\sin(\phi_{56}) - |t_7||t_8|\sin(\phi_{78})$	$\langle t|\Gamma_{s3}^{III}|t\rangle$	$\mathcal{O}_{yx'}$
$\mathcal{O}_{s4}^{III}$	$|t_1||t_2|\sin(\phi_{12}) - |t_3||t_4|\sin(\phi_{34}) - |t_5||t_6|\sin(\phi_{56}) + |t_7||t_8|\sin(\phi_{78})$	$\langle t|\Gamma_{s4}^{III}|t\rangle$	$\mathcal{O}_{yx'}^{\odot}$
$\mathcal{O}_{c1}^{IV}$	$|t_1||t_4|\cos(\phi_{14}) + |t_2||t_3|\cos(\phi_{23}) + |t_5||t_8|\cos(\phi_{58}) + |t_6||t_7|\cos(\phi_{67})$	$\langle t|\Gamma_{c1}^{IV}|t\rangle$	$\mathcal{O}_{zz'}$
$\mathcal{O}_{c2}^{IV}$	$|t_1||t_4|\cos(\phi_{14}) + |t_2||t_3|\cos(\phi_{23}) - |t_5||t_8|\cos(\phi_{58}) - |t_6||t_7|\cos(\phi_{67})$	$\langle t|\Gamma_{c2}^{IV}|t\rangle$	$\mathcal{O}_{zz'}^{\odot}$
$\mathcal{O}_{c3}^{IV}$	$|t_1||t_4|\cos(\phi_{14}) - |t_2||t_3|\cos(\phi_{23}) + |t_5||t_8|\cos(\phi_{58}) - |t_6||t_7|\cos(\phi_{67})$	$\langle t|\Gamma_{c3}^{IV}|t\rangle$	$\mathcal{O}_{xx'}$
$\mathcal{O}_{c4}^{IV}$	$|t_1||t_4|\cos(\phi_{14}) - |t_2||t_3|\cos(\phi_{23}) - |t_5||t_8|\cos(\phi_{58}) + |t_6||t_7|\cos(\phi_{67})$	$\langle t|\Gamma_{c4}^{IV}|t\rangle$	$\mathcal{O}_{xx'}^{\odot}$
$\mathcal{O}_{s1}^{IV}$	$|t_1||t_4|\sin(\phi_{14}) + |t_2||t_3|\sin(\phi_{23}) + |t_5||t_8|\sin(\phi_{58}) + |t_6||t_7|\sin(\phi_{67})$	$\langle t|\Gamma_{s1}^{IV}|t\rangle$	$\mathcal{O}_{xz'}$
$\mathcal{O}_{s2}^{IV}$	$|t_1||t_4|\sin(\phi_{14}) + |t_2||t_3|\sin(\phi_{23}) - |t_5||t_8|\sin(\phi_{58}) - |t_6||t_7|\sin(\phi_{67})$	$\langle t|\Gamma_{s2}^{IV}|t\rangle$	$\mathcal{O}_{xz'}^{\odot}$
$\mathcal{O}_{s3}^{IV}$	$|t_1||t_4|\sin(\phi_{14}) - |t_2||t_3|\sin(\phi_{23}) + |t_5||t_8|\sin(\phi_{58}) - |t_6||t_7|\sin(\phi_{67})$	$\langle t|\Gamma_{s3}^{IV}|t\rangle$	$-\mathcal{O}_{zx'}$
$\mathcal{O}_{s4}^{IV}$	$|t_1||t_4|\sin(\phi_{14}) - |t_2||t_3|\sin(\phi_{23}) - |t_5||t_8|\sin(\phi_{58}) + |t_6||t_7|\sin(\phi_{67})$	$\langle t|\Gamma_{s4}^{IV}|t\rangle$	$-\mathcal{O}_{zx'}^{\odot}$
$\mathcal{O}_{c1}^{V}$	$|t_1||t_5|\cos(\phi_{15}) + |t_2||t_6|\cos(\phi_{26}) + |t_3||t_7|\cos(\phi_{37}) + |t_4||t_8|\cos(\phi_{48})$	$\langle t|\Gamma_{c1}^{V}|t\rangle$	$-I^c$
$\mathcal{O}_{c2}^{V}$	$|t_1||t_5|\cos(\phi_{15}) + |t_2||t_6|\cos(\phi_{26}) - |t_3||t_7|\cos(\phi_{37}) - |t_4||t_8|\cos(\phi_{48})$	$\langle t|\Gamma_{c2}^{V}|t\rangle$	$-P_y^c$
$\mathcal{O}_{c3}^{V}$	$|t_1||t_5|\cos(\phi_{15}) - |t_2||t_6|\cos(\phi_{26}) + |t_3||t_7|\cos(\phi_{37}) - |t_4||t_8|\cos(\phi_{48})$	$\langle t|\Gamma_{c3}^{V}|t\rangle$	$-P_{y'}^c$
$\mathcal{O}_{c4}^{V}$	$|t_1||t_5|\cos(\phi_{15}) - |t_2||t_6|\cos(\phi_{26}) - |t_3||t_7|\cos(\phi_{37}) + |t_4||t_8|\cos(\phi_{48})$	$\langle t|\Gamma_{c4}^{V}|t\rangle$	$-\mathcal{O}_{yy'}^c$
$\mathcal{O}_{s1}^{V}$	$|t_1||t_5|\sin(\phi_{15}) + |t_2||t_6|\sin(\phi_{26}) + |t_3||t_7|\sin(\phi_{37}) + |t_4||t_8|\sin(\phi_{48})$	$\langle t|\Gamma_{s1}^{V}|t\rangle$	$-I^s$
$\mathcal{O}_{s2}^{V}$	$|t_1||t_5|\sin(\phi_{15}) + |t_2||t_6|\sin(\phi_{26}) - |t_3||t_7|\sin(\phi_{37}) - |t_4||t_8|\sin(\phi_{48})$	$\langle t|\Gamma_{s2}^{V}|t\rangle$	$-P_y^s$
$\mathcal{O}_{s3}^{V}$	$|t_1||t_5|\sin(\phi_{15}) - |t_2||t_6|\sin(\phi_{26}) + |t_3||t_7|\sin(\phi_{37}) - |t_4||t_8|\sin(\phi_{48})$	$\langle t|\Gamma_{s3}^{V}|t\rangle$	$-P_{y'}^s$
$\mathcal{O}_{s4}^{V}$	$|t_1||t_5|\sin(\phi_{15}) - |t_2||t_6|\sin(\phi_{26}) - |t_3||t_7|\sin(\phi_{37}) + |t_4||t_8|\sin(\phi_{48})$	$\langle t|\Gamma_{s4}^{V}|t\rangle$	$-\mathcal{O}_{yy'}^s$
$\mathcal{O}_{c1}^{VI}$	$|t_1||t_7|\cos(\phi_{17}) + |t_2||t_8|\cos(\phi_{28}) + |t_3||t_5|\cos(\phi_{35}) + |t_4||t_6|\cos(\phi_{46})$	$\langle t|\Gamma_{c1}^{VI}|t\rangle$	P_z^c
$\mathcal{O}_{c2}^{VI}$	$|t_1||t_7|\cos(\phi_{17}) + |t_2||t_8|\cos(\phi_{28}) - |t_3||t_5|\cos(\phi_{35}) - |t_4||t_6|\cos(\phi_{46})$	$\langle t|\Gamma_{c2}^{VI}|t\rangle$	$-P_x^s$
$\mathcal{O}_{c3}^{VI}$	$|t_1||t_7|\cos(\phi_{17}) - |t_2||t_8|\cos(\phi_{28}) + |t_3||t_5|\cos(\phi_{35}) - |t_4||t_6|\cos(\phi_{46})$	$\langle t|\Gamma_{c3}^{VI}|t\rangle$	$\mathcal{O}_{zy'}^c$
$\mathcal{O}_{c4}^{VI}$	$|t_1||t_7|\cos(\phi_{17}) - |t_2||t_8|\cos(\phi_{28}) - |t_3||t_5|\cos(\phi_{35}) + |t_4||t_6|\cos(\phi_{46})$	$\langle t|\Gamma_{c4}^{VI}|t\rangle$	$-\mathcal{O}_{xy'}^s$
$\mathcal{O}_{s1}^{VI}$	$|t_1||t_7|\sin(\phi_{17}) + |t_2||t_8|\sin(\phi_{28}) + |t_3||t_5|\sin(\phi_{35}) + |t_4||t_6|\sin(\phi_{46})$	$\langle t|\Gamma_{s1}^{VI}|t\rangle$	P_z^s
$\mathcal{O}_{s2}^{VI}$	$|t_1||t_7|\sin(\phi_{17}) + |t_2||t_8|\sin(\phi_{28}) - |t_3||t_5|\sin(\phi_{35}) - |t_4||t_6|\sin(\phi_{46})$	$\langle t|\Gamma_{s2}^{VI}|t\rangle$	P_x^c
$\mathcal{O}_{s3}^{VI}$	$|t_1||t_7|\sin(\phi_{17}) - |t_2||t_8|\sin(\phi_{28}) + |t_3||t_5|\sin(\phi_{35}) - |t_4||t_6|\sin(\phi_{46})$	$\langle t|\Gamma_{s3}^{VI}|t\rangle$	$\mathcal{O}_{zy'}^s$
$\mathcal{O}_{s4}^{VI}$	$|t_1||t_7|\sin(\phi_{17}) - |t_2||t_8|\sin(\phi_{28}) - |t_3||t_5|\sin(\phi_{35}) + |t_4||t_6|\sin(\phi_{46})$	$\langle t|\Gamma_{s4}^{VI}|t\rangle$	$\mathcal{O}_{xy'}^c$
$\mathcal{O}_{c1}^{VII}$	$|t_1||t_6|\cos(\phi_{16}) + |t_2||t_5|\cos(\phi_{25}) + |t_3||t_8|\cos(\phi_{38}) + |t_4||t_7|\cos(\phi_{47})$	$\langle t|\Gamma_{c1}^{VII}|t\rangle$	$P_{z'}^c$
$\mathcal{O}_{c2}^{VII}$	$|t_1||t_6|\cos(\phi_{16}) + |t_2||t_5|\cos(\phi_{25}) - |t_3||t_8|\cos(\phi_{38}) - |t_4||t_7|\cos(\phi_{47})$	$\langle t|\Gamma_{c2}^{VII}|t\rangle$	$\mathcal{O}_{yz'}^c$
$\mathcal{O}_{c3}^{VII}$	$|t_1||t_6|\cos(\phi_{16}) - |t_2||t_5|\cos(\phi_{25}) + |t_3||t_8|\cos(\phi_{38}) - |t_4||t_7|\cos(\phi_{47})$	$\langle t|\Gamma_{c3}^{VII}|t\rangle$	$P_{x'}^s$
$\mathcal{O}_{c4}^{VII}$	$|t_1||t_6|\cos(\phi_{16}) - |t_2||t_5|\cos(\phi_{25}) - |t_3||t_8|\cos(\phi_{38}) + |t_4||t_7|\cos(\phi_{47})$	$\langle t|\Gamma_{c4}^{VII}|t\rangle$	$\mathcal{O}_{yx'}^s$

TABLE I. *(Continued.)*

Observable	Definition in terms of polar coordinates / 2	Bilinear form	Roberts, Oed
$\mathcal{O}_{s1}^{VII}$	$|t_1||t_6|\sin(\phi_{16}) + |t_2||t_5|\sin(\phi_{25}) + |t_3||t_8|\sin(\phi_{38}) + |t_4||t_7|\sin(\phi_{47})$	$\langle t|\Gamma_{s1}^{VII}|t\rangle$	$P_{z'}^s$
$\mathcal{O}_{s2}^{VII}$	$|t_1||t_6|\sin(\phi_{16}) + |t_2||t_5|\sin(\phi_{25}) - |t_3||t_8|\sin(\phi_{38}) - |t_4||t_7|\sin(\phi_{47})$	$\langle t|\Gamma_{s2}^{VII}|t\rangle$	$\mathcal{O}_{yz'}^s$
$\mathcal{O}_{s3}^{VII}$	$|t_1||t_6|\sin(\phi_{16}) - |t_2||t_5|\sin(\phi_{25}) + |t_3||t_8|\sin(\phi_{38}) - |t_4||t_7|\sin(\phi_{47})$	$\langle t|\Gamma_{s3}^{VII}|t\rangle$	$-P_{x'}^s$
$\mathcal{O}_{s4}^{VII}$	$|t_1||t_6|\sin(\phi_{16}) - |t_2||t_5|\sin(\phi_{25}) - |t_3||t_8|\sin(\phi_{38}) + |t_4||t_7|\sin(\phi_{47})$	$\langle t|\Gamma_{s4}^{VII}|t\rangle$	$-\mathcal{O}_{yx'}^c$
$\mathcal{O}_{c1}^{VIII}$	$|t_1||t_8|\cos(\phi_{18}) + |t_2||t_7|\cos(\phi_{27}) + |t_3||t_6|\cos(\phi_{36}) + |t_4||t_5|\cos(\phi_{45})$	$\langle t|\Gamma_{c1}^{VIII}|t\rangle$	$-\mathcal{O}_{zz'}^c$
$\mathcal{O}_{c2}^{VIII}$	$|t_1||t_8|\cos(\phi_{18}) + |t_2||t_7|\cos(\phi_{27}) - |t_3||t_6|\cos(\phi_{36}) - |t_4||t_5|\cos(\phi_{45})$	$\langle t|\Gamma_{c2}^{VIII}|t\rangle$	$\mathcal{O}_{xz'}^s$
$\mathcal{O}_{c3}^{VIII}$	$|t_1||t_8|\cos(\phi_{18}) - |t_2||t_7|\cos(\phi_{27}) + |t_3||t_6|\cos(\phi_{36}) - |t_4||t_5|\cos(\phi_{45})$	$\langle t|\Gamma_{c3}^{VIII}|t\rangle$	$-\mathcal{O}_{zx'}^s$
$\mathcal{O}_{c4}^{VIII}$	$|t_1||t_8|\cos(\phi_{18}) - |t_2||t_7|\cos(\phi_{27}) - |t_3||t_6|\cos(\phi_{36}) + |t_4||t_5|\cos(\phi_{45})$	$\langle t|\Gamma_{c4}^{VIII}|t\rangle$	$-\mathcal{O}_{xx'}^c$
$\mathcal{O}_{s1}^{VIII}$	$|t_1||t_8|\sin(\phi_{18}) + |t_2||t_7|\sin(\phi_{27}) + |t_3||t_6|\sin(\phi_{36}) + |t_4||t_5|\sin(\phi_{45})$	$\langle t|\Gamma_{s1}^{VIII}|t\rangle$	$-\mathcal{O}_{zz'}^s$
$\mathcal{O}_{s2}^{VIII}$	$|t_1||t_8|\sin(\phi_{18}) + |t_2||t_7|\sin(\phi_{27}) - |t_3||t_6|\sin(\phi_{36}) - |t_4||t_5|\sin(\phi_{45})$	$\langle t|\Gamma_{s2}^{VIII}|t\rangle$	$-\mathcal{O}_{xz'}^c$
$\mathcal{O}_{s3}^{VIII}$	$|t_1||t_8|\sin(\phi_{18}) - |t_2||t_7|\sin(\phi_{27}) + |t_3||t_6|\sin(\phi_{36}) - |t_4||t_5|\sin(\phi_{45})$	$\langle t|\Gamma_{s3}^{VIII}|t\rangle$	$\mathcal{O}_{zx'}^c$
$\mathcal{O}_{s4}^{VIII}$	$|t_1||t_8|\sin(\phi_{18}) - |t_2||t_7|\sin(\phi_{27}) - |t_3||t_6|\sin(\phi_{36}) + |t_4||t_5|\sin(\phi_{45})$	$\langle t|\Gamma_{s4}^{VIII}|t\rangle$	$-\mathcal{O}_{xx'}^s$

TABLE II. Definition of the 64 Γ matrices in terms of the well-known Pauli matrices in combination with the Kronecker product. The gray shaded cells within the column "Shape-class" correspond to the nonzero matrix entries.

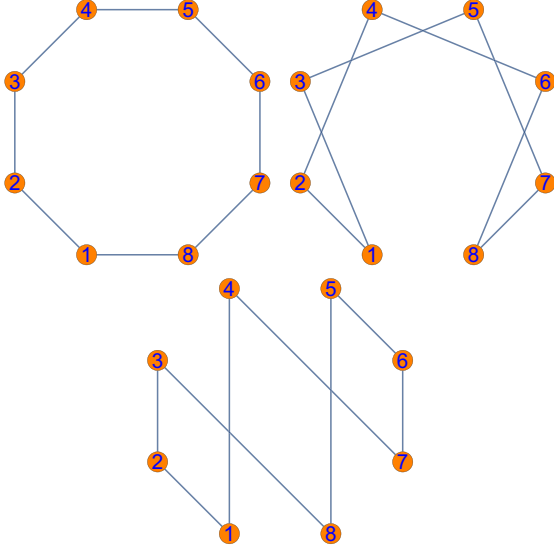| Γ-matrices	Definition	Shape-class	Γ-matrices	Definition	Shape-class
Γ_1^I	$\sigma^3 \otimes I_2 \otimes I_2$		Γ_{c1}^V	$\sigma^1 \otimes I_2 \otimes I_2$	
Γ_2^I	$I_2 \otimes \sigma^3 \otimes I_2$		Γ_{c2}^V	$\sigma^1 \otimes \sigma^3 \otimes I_2$	
Γ_3^I	$I_2 \otimes I_2 \otimes \sigma^3$		Γ_{c3}^V	$\sigma^1 \otimes I_2 \otimes \sigma^3$	
Γ_4^I	$\sigma^3 \otimes \sigma^3 \otimes \sigma^3$		Γ_{c4}^V	$\sigma^1 \otimes \sigma^3 \otimes \sigma^3$	
Γ_5^I	$I_2 \otimes \sigma^3 \otimes \sigma^3$		Γ_{s1}^V	$-\sigma^2 \otimes I_2 \otimes I_2$	
Γ_6^I	$\sigma^3 \otimes I_2 \otimes \sigma^3$		Γ_{s2}^V	$-\sigma^2 \otimes \sigma^3 \otimes I_2$	
Γ_7^I	$\sigma^3 \otimes \sigma^3 \otimes I_2$		Γ_{s3}^V	$-\sigma^2 \otimes I_2 \otimes \sigma^3$	
Γ_8^I	$I_2 \otimes I_2 \otimes I_2$		Γ_{s4}^V	$-\sigma^2 \otimes \sigma^3 \otimes \sigma^3$	
Γ_{c1}^{II}	$I_2 \otimes \sigma^1 \otimes I_2$		Γ_{c1}^{VI}	$\sigma^1 \otimes \sigma^1 \otimes I_2$	
Γ_{c2}^{II}	$\sigma^3 \otimes \sigma^1 \otimes I_2$		Γ_{c2}^{VI}	$-\sigma^2 \otimes \sigma^2 \otimes I_2$	
Γ_{c3}^{II}	$I_2 \otimes \sigma^1 \otimes \sigma^3$		Γ_{c3}^{VI}	$\sigma^1 \otimes \sigma^1 \otimes \sigma^3$	
Γ_{c4}^{II}	$\sigma^3 \otimes \sigma^1 \otimes \sigma^3$		Γ_{c4}^{VI}	$-\sigma^2 \otimes \sigma^2 \otimes \sigma^3$	
Γ_{s1}^{II}	$-I_2 \otimes \sigma^2 \otimes I_2$		Γ_{s1}^{VI}	$-\sigma^2 \otimes \sigma^1 \otimes I_2$	
Γ_{s2}^{II}	$-\sigma^3 \otimes \sigma^2 \otimes I_2$		Γ_{s2}^{VI}	$-\sigma^1 \otimes \sigma^2 \otimes I_2$	
Γ_{s3}^{II}	$-I_2 \otimes \sigma^2 \otimes \sigma^3$		Γ_{s3}^{VI}	$-\sigma^2 \otimes \sigma^1 \otimes \sigma^3$	
Γ_{s4}^{II}	$-\sigma^3 \otimes \sigma^2 \otimes \sigma^3$		Γ_{s4}^{VI}	$-\sigma^1 \otimes \sigma^2 \otimes \sigma^3$	
Γ_{c1}^{III}	$I_2 \otimes I_2 \otimes \sigma^1$		Γ_{c1}^{VII}	$\sigma^1 \otimes I_2 \otimes \sigma^1$	
Γ_{c2}^{III}	$\sigma^3 \otimes I_2 \otimes \sigma^1$		Γ_{c2}^{VII}	$\sigma^1 \otimes \sigma^3 \otimes \sigma^1$	
Γ_{c3}^{III}	$I_2 \otimes \sigma^3 \otimes \sigma^1$		Γ_{c3}^{VII}	$-\sigma^2 \otimes I_2 \otimes \sigma^2$	
Γ_{c4}^{III}	$\sigma^3 \otimes \sigma^3 \otimes \sigma^1$		Γ_{c4}^{VII}	$-\sigma^2 \otimes \sigma^3 \otimes \sigma^2$	
Γ_{s1}^{III}	$-I_2 \otimes I_2 \otimes \sigma^2$		Γ_{s1}^{VII}	$-\sigma^2 \otimes I_2 \otimes \sigma^1$	
Γ_{s2}^{III}	$-\sigma^3 \otimes I_2 \otimes \sigma^2$		Γ_{s2}^{VII}	$-\sigma^2 \otimes \sigma^3 \otimes \sigma^1$	
Γ_{s3}^{III}	$-I_2 \otimes \sigma^3 \otimes \sigma^2$		Γ_{s3}^{VII}	$-\sigma^1 \otimes I_2 \otimes \sigma^2$	
Γ_{s4}^{III}	$-\sigma^3 \otimes \sigma^3 \otimes \sigma^2$		Γ_{s4}^{VII}	$-\sigma^1 \otimes \sigma^3 \otimes \sigma^2$	
Γ_{c1}^{IV}	$I_2 \otimes \sigma^1 \otimes \sigma^1$		Γ_{c1}^{VIII}	$\sigma^1 \otimes \sigma^1 \otimes \sigma^1$	
Γ_{c2}^{IV}	$\sigma^3 \otimes \sigma^1 \otimes \sigma^1$		Γ_{c2}^{VIII}	$-\sigma^2 \otimes \sigma^2 \otimes \sigma^1$	
Γ_{c3}^{IV}	$-I_2 \otimes \sigma^2 \otimes \sigma^2$		Γ_{c3}^{VIII}	$-\sigma^2 \otimes \sigma^1 \otimes \sigma^2$	
Γ_{c4}^{IV}	$-\sigma^3 \otimes \sigma^2 \otimes \sigma^2$		Γ_{c4}^{VIII}	$-\sigma^1 \otimes \sigma^2 \otimes \sigma^2$	
Γ_{s1}^{IV}	$-I_2 \otimes \sigma^2 \otimes \sigma^1$		Γ_{s1}^{VIII}	$-\sigma^2 \otimes \sigma^1 \otimes \sigma^1$	
Γ_{s2}^{IV}	$-\sigma^3 \otimes \sigma^2 \otimes \sigma^1$		Γ_{s2}^{VIII}	$-\sigma^1 \otimes \sigma^2 \otimes \sigma^1$	
Γ_{s3}^{IV}	$-I_2 \otimes \sigma^1 \otimes \sigma^2$		Γ_{s3}^{VIII}	$-\sigma^1 \otimes \sigma^1 \otimes \sigma^2$	
Γ_{s4}^{IV}	$-\sigma^3 \otimes \sigma^1 \otimes \sigma^2$		Γ_{s4}^{VIII}	$\sigma^2 \otimes \sigma^2 \otimes \sigma^2$	

FIG. 2. Examples of graph topologies. Only three out of 2520 unique cycle graphs with eight nodes are shown.

In a second step, all possible edge configurations which yield a complete set of observables are constructed. An example is shown in Fig. 1. This is done for each unique topology. The total number of possible edge configurations can be calculated by $\sum_{k=1}^{N} \binom{N}{k}$ for all odd $k \leqslant N$.

The final step involves the mapping from bilinear forms to the actual observables. Referring again to the example in Fig. 1, the overall question is which combinations of observables can be solely described by these bilinear products (given that all amplitudes are known)? Considering Table I, the following relations are evident:

$$\sin(\phi_{12}) \mapsto \{\mathcal{O}_{s1}^{III}, \mathcal{O}_{s2}^{III}, \mathcal{O}_{s3}^{III}, \mathcal{O}_{s4}^{III}\}, \tag{6}$$

$$\sin(\phi_{34}) \mapsto \{\mathcal{O}_{s1}^{III}, \mathcal{O}_{s2}^{III}, \mathcal{O}_{s3}^{III}, \mathcal{O}_{s4}^{III}\}, \tag{7}$$

$$\sin(\phi_{56}) \mapsto \{\mathcal{O}_{s1}^{III}, \mathcal{O}_{s2}^{III}, \mathcal{O}_{s3}^{III}, \mathcal{O}_{s4}^{III}\}, \tag{8}$$

$$\sin(\phi_{78}) \mapsto \{\mathcal{O}_{s1}^{III}, \mathcal{O}_{s2}^{III}, \mathcal{O}_{s3}^{III}, \mathcal{O}_{s4}^{III}\} \tag{9}$$

$$\sin(\phi_{14}) \mapsto \{\mathcal{O}_{s1}^{IV}, \mathcal{O}_{s2}^{IV}, \mathcal{O}_{s3}^{IV}, \mathcal{O}_{s4}^{IV}\}, \tag{10}$$

$$\sin(\phi_{58}) \mapsto \{\mathcal{O}_{s1}^{IV}, \mathcal{O}_{s2}^{IV}, \mathcal{O}_{s3}^{IV}, \mathcal{O}_{s4}^{IV}\}, \tag{11}$$

$$\sin(\phi_{27}) \mapsto \{\mathcal{O}_{s1}^{VIII}, \mathcal{O}_{s2}^{VIII}, \mathcal{O}_{s3}^{VIII}, \mathcal{O}_{s4}^{VIII}\}, \tag{12}$$

$$\cos(\phi_{36}) \mapsto \{\mathcal{O}_{c1}^{VIII}, \mathcal{O}_{c2}^{VIII}, \mathcal{O}_{c3}^{VIII}, \mathcal{O}_{c4}^{VIII}\}. \tag{13}$$

Thus, the complete set of observables which corresponds to the graph configuration shown in Fig. 1 is

$$\{\mathcal{O}_1^{I}, \mathcal{O}_2^{I}, \mathcal{O}_3^{I}, \mathcal{O}_4^{I}, \mathcal{O}_5^{I}, \mathcal{O}_6^{I}, \mathcal{O}_7^{I}, \mathcal{O}_8^{I},$$
$$\mathcal{O}_{s1}^{III}, \mathcal{O}_{s2}^{III}, \mathcal{O}_{s3}^{III}, \mathcal{O}_{s4}^{III}, \mathcal{O}_{s1}^{IV}, \mathcal{O}_{s2}^{IV}, \mathcal{O}_{s3}^{IV}, \mathcal{O}_{s4}^{IV},$$
$$\mathcal{O}_{s1}^{VIII}, \mathcal{O}_{s2}^{VIII}, \mathcal{O}_{s3}^{VIII}, \mathcal{O}_{s4}^{VIII}, \mathcal{O}_{c1}^{VIII}, \mathcal{O}_{c2}^{VIII}, \mathcal{O}_{c3}^{VIII}, \mathcal{O}_{c4}^{VIII}\}. \tag{14}$$

In general one needs to add the observables which are solely described by moduli in order to fix the moduli of the complex

TABLE III. The 64 observables are grouped into eight categories according to the polarization needed to measure these observables (beam $\mathcal{B}$, target $\mathcal{T}$, and recoil $\mathcal{R}$). The notation used in the original paper of Roberts and Oed [5] is used for the observables. The observable I_0 corresponds to the unpolarized cross section.

Category	Subcategory	Observables
		I_0
$\mathcal{B}$	$\mathcal{B}_1$	I^s, I^c
	$\mathcal{B}_\odot$	$I^\odot$
$\mathcal{T}$		P_x, P_y, P_z
$\mathcal{R}$		$P_{x'}, P_{y'}, P_{z'}$
$\mathcal{BT}$	$\mathcal{B}_1\mathcal{T}$	$P_x^s, P_y^s, P_z^s, P_x^c, P_y^c, P_z^c$
	$\mathcal{B}_\odot\mathcal{T}$	$P_x^\odot, P_y^\odot, P_z^\odot$
$\mathcal{BR}$	$\mathcal{B}_1\mathcal{R}$	$P_{x'}^s, P_{y'}^s, P_{z'}^s, P_{x'}^c, P_{y'}^c, P_{z'}^c$
	$\mathcal{B}_\odot\mathcal{R}$	$P_{x'}^\odot, P_{y'}^\odot, P_{z'}^\odot$
$\mathcal{TR}$		$\mathcal{O}_{xx'}, \mathcal{O}_{xy'}, \mathcal{O}_{xz'}, \mathcal{O}_{yx'}, \mathcal{O}_{yy'}, \mathcal{O}_{yz'}, \mathcal{O}_{zx'}$
		$\mathcal{O}_{zy'}, \mathcal{O}_{zz'}$
$\mathcal{BTR}$	$\mathcal{B}_1\mathcal{TR}$	$\mathcal{O}_{xx'}^s, \mathcal{O}_{xy'}^s, \mathcal{O}_{xz'}^s, \mathcal{O}_{yx'}^s, \mathcal{O}_{yy'}^s, \mathcal{O}_{yz'}^s, \mathcal{O}_{zx'}^s$
		$\mathcal{O}_{zy'}^s, \mathcal{O}_{zz'}^s$
		$\mathcal{O}_{xx'}^c, \mathcal{O}_{xy'}^c, \mathcal{O}_{xz'}^c, \mathcal{O}_{yx'}^c, \mathcal{O}_{yy'}^c, \mathcal{O}_{yz'}^c, \mathcal{O}_{zx'}^c$
		$\mathcal{O}_{zy'}^c, \mathcal{O}_{zz'}^c$
	$\mathcal{B}_\odot\mathcal{TR}$	$\mathcal{O}_{xx'}^\odot, \mathcal{O}_{xy'}^\odot, \mathcal{O}_{xz'}^\odot, \mathcal{O}_{yx'}^\odot, \mathcal{O}_{yy'}^\odot, \mathcal{O}_{yz'}^\odot, \mathcal{O}_{zx'}^\odot$
		$\mathcal{O}_{zy'}^\odot, \mathcal{O}_{zz'}^\odot$

amplitudes t_i (see Sec. II). In this case, these are the group I observables, as shown in Table I. Thus, Eq. (14) accounts for a total of 24 observables.

The same result can be obtained by using the relation:

$$t_j^* t_i = \frac{1}{8} \sum_{\alpha=1}^{64} \Gamma_{ij}^\alpha \mathcal{O}^\alpha, \tag{15}$$

where α is an index running through the observables listed in Table I and the Γ matrices as listed in Table II. Equation (15) is derived by using $\mathcal{O}^\alpha = \sum_{i,j=1}^{8} t_i^* \Gamma_{ij}^\alpha t_j$ in combination with the completeness relation of the Γ matrices $\sum_{\alpha=1}^{64} \Gamma_{ai}^\alpha \Gamma_{jb}^\alpha = 8\delta_{ab}\delta_{ij}$.

V. DATABASE FOR TWO PSEUDOSCALAR MESON PHOTOPRODUCTION

As already mentioned, 64 observables can be measured for two pseudoscalar meson photoproduction using the full three-body kinematics of the reaction. These observables can be organized into three groups: single, double, and triple polarization observables, which require either the use of a polarized beam $\mathcal{B}$, a polarized target $\mathcal{T}$, a recoil polarimeter $\mathcal{R}$, or a combination of the three. Table III gives an overview of all the observables of each category. In addition to the unpolarized cross section I_0, there are three observables in each single polarization observable category ($\mathcal{B}, \mathcal{T}, \mathcal{R}$), nine in each double polarization observable category ($\mathcal{BT}, \mathcal{BR}$, and $\mathcal{TR}$) and 27 observables in the triple polarization observable category ($\mathcal{BTR}$).

The description of the full three-body kinematics requires five independent variables [14]. In this context, two planes,

the reaction plane and the decay plane, are often used [14,15]. While the reaction plane is defined by the incoming photon and one of the outgoing particles, the decay plane is spanned by the other two outgoing particles. The angle between the reaction and the decay plane is called ϕ^*. Integrating over ϕ^* makes it possible to treat the three-body final state as a two-body final state, resulting in a reduced number of observables. In this case, the observables correspond to observables known from single meson photoproduction [7], e.g., category $\mathcal{B}$ reduces to $I^c = \Sigma$, category $\mathcal{T}$ to $P_y = T$, category $\mathcal{R}$ to $P_{y'} = P$ (this observable can be also measured as a double polarization observable $-P_x^c$ [5]), and category $\mathcal{BT}$ to $P_x^s = H$, $P_z^s = G$, $P_x^\odot = F$, and $P_z^\odot = E$ [5].

In the case of single pseudoscalar meson photoproduction, quite a lot measurements were performed to determine single and double polarization observables. An extensive overview over the performed measurements, on the basis of the SAID database [16], was brought together recently by Ireland, Pasyuk, and Strakovsky [17].

A similar database does not exist yet for double pseudoscalar meson photoproduction. Thus, for the first time, an extensive overview of measurements of polarization observables for double pseudoscalar meson photoproduction is presented in Table IV.

By far the most measurements where performed for the reaction $\gamma p \to p\pi^0\pi^0$ because the reaction has the least amount of nonresonant background amplitude contributions compared with other isospin channels [1]. The most common observable is the unpolarized cross section I_0, followed by the beam asymmetries I^s, I^c, and $I^\odot$. Even a few double polarization observables in quasi-two-body kinematics were measured, i.e., E and H. Until now, no triple polarization observables were extracted, as it is experimentally challenging to measure the polarization of a recoiling particle [18,19] in addition to a polarized beam and a polarized target.

However, a few words of caution are in order. One might get the impression of a huge existing database with plenty of data. It should be kept in mind that the data entries span more than half a century, thus including data with lower-performing experimental setups in comparison with the latest published polarization observables data. The collection consists mainly of measurements concerning the unpolarized cross section I_0 (roughly 60%). Taken as a whole, the current database is not sufficient for an experimental verification of a complete experiment analysis. This issue is further discussed in Sec. VIII for experimentalists. But also for theoreticians using phenomenological models to fit and interpret the data, it is challenging and necessary to check the different data sets for consistency between different experiments and to deal with the systematic uncertainties of the data.

VI. RESULTS FOR $N = 8$

For $N = 8$ one has 2520 unique cycle graphs, each with 128 unique edge configurations, as explained in Sec. IV. Hence, there exist in total $128 \times 2520 = 322\,560$ edge configurations which yield a complete set of observables. However, the resulting sets are not all linearly independent.

The whole algorithm was implemented in *Mathematica* [56], but can just as easily be implemented in other languages such as JULIA [57]. Filtering out the redundant sets, one is left with 5964 unique sets of observables. The length of the sets varies between the topologies as well as between different edge configurations. To be exact, it varies between a total of 24 and 40 observables.

Without loss of generality, the further analysis focuses on the 392 distinct sets with 24 observables. A numerical analysis was performed which showed that these sets are indeed complete. The applied algorithm is described in Appendix.

Further characteristics of the minimal sets according to Moravcsik involve the following:

(i) Each set inhibits at least five triple polarization observables.
(ii) The sets are constructed from four or five different shape classes.

However, these sets are slightly overcomplete since each observable depends on more than one bilinear product. According to current knowledge [11,13], a truly minimal complete set consists of $2N$ observables. Thus the task remains to reduce the slightly overcomplete sets by eight observables while retaining completeness.

VII. REDUCTION TO MINIMAL SETS OF $2N$

A. Numerical calculation

The smallest complete sets, which emerge from the modified version of Moravcsik's theorem, have a length of 24 (for $N = 8$). Eight of these observables cannot be omitted, namely, the group I observables, as discussed in Sec. IV. From the remaining 16 observables one constructs all possible subsets containing eight observables, which amounts to $\binom{16}{8} = 12\,870$ distinct sets.

In principle this is done for all sets with a length of 24, leading to just over five million minimal, complete set candidates. This number can be further reduced by $\approx 0.7\%$, by noting that sets containing only one or two distinct observable groups (apart from group I) do not correspond to a connected graph and thus do not form a complete set. There are also a few cases in which three distinct observable groups (apart from group I) are not able to form a connected graph, i.e., {II,III,IV}, {II,V,VI}, {II,VII,VIII}, {III,V,VII}, {III,VI,VIII}, {IV,V,VIII}, and {IV,VI,VII}.

However, due to the enormous number of possible candidate sets, just a minor excerpt was analyzed for this paper. The sets of interest are checked for completeness via a numerical analysis. The employed algorithm is described in Appendix.

So far, 4185 unique truly minimal sets of length $2N = 16$ have been found. There are two major differences to the slightly overcomplete sets with 24 observables. On the one hand, all sets found are constructed from exactly four different shape classes. On the other hand, truly minimal complete sets exist with a minimal number of triple polarization observables, namely only $\mathcal{O}_4^I = \mathcal{O}_{yy'}^\odot$ from group I. Hence, this observable has to be included in every set as explained in Sec. II.

TABLE IV. A collection of polarization observable measurements for two pseudoscalar meson photoproduction. Hint: We do not distinguish the datasets according to the kinematical variable and whether is differential or total cross-section data. Further details can be found in the cited references.

Observable	Energy range E_γ^{lab}	Facility	Reference	Year of publication
		$\gamma p \rightarrow p\pi^0\pi^0$		
I_0	309–792 MeV	TAPS at MAMI	Härter *et al.* [20]	1997
I_0	309–820 MeV	TAPS at MAMI	Wolf *et al.* [21]	2000
I_0	200–820 MeV	TAPS at MAMI	Kleber *et al.* [22]	2000
I_0	300–425 MeV	TAPS at MAMI	Kotulla *et al.* [23]	2004
I_0	309–800 MeV	CB/TAPS at MAMI	Zehr *et al.* [24]	2012
I_0	309–1400 MeV	CB/TAPS at MAMI	Kashevarov *et al.* [25]	2012
I_0	432–1374 MeV	CB/TAPS at MAMI	Dieterle *et al.* [26]	2015
I_0	400–800 MeV	DAPHNE at MAMI	Braghieri *et al.* [27]	1995
I_0	400–800 MeV	DAPHNE at MAMI	Ahrens *et al.* [28]	2005
I_0	309–820 MeV	TAPS at MAMI, CB at ELSA	Sarantsev *et al.* [29]	2008
I_0	400–1300 MeV	CB at ELSA	Thoma *et al.* [30]	2008
I_0	≈750–2500 MeV	CBELSA/TAPS at ELSA	Thiel *et al.* [31]	2015
I_0, Σ	600–2500 MeV	CB/TAPS at ELSA	Sokhoyan *et al.* [1]	2015
I_0, Σ	650–1450 MeV	GRAAL	Assafiri *et al.* [32]	2003
Σ	650–1450 MeV	CB at ELSA	Thoma *et al.* [30]	2008
$I^\odot$	560–810 MeV	CB/TAPS at MAMI	Krambrich *et al.* [33]	2009
$I^\odot$	≈600–1400 MeV	CB/TAPS at MAMI	Oberle *et al.* [34]	2013
$I^\odot$	550–820 MeV	CB/TAPS at MAMI	Zehr *et al.* [24]	2012
E, $\sigma_{1/2}$, $\sigma_{3/2}$	≈431–1455 MeV	CB/TAPS at MAMI	Dieterle *et al.* [35]	2020
P_x, P_y, T, H, P	650–2600 MeV	CBELSA/TAPS at ELSA	Seifen *et al.* [14]	2020
I^c, I^s	970–1650 MeV	CB/TAPS at ELSA	Sokhoyan *et al.* [1]	2015
		$\gamma p \rightarrow p\pi^+\pi^-$		
I_0	400–800 MeV	DAPHNE at MAMI	Braghieri *et al.* [27]	1995
I_0	400–800 MeV	DAPHNE at MAMI	Ahrens *et al.* [36]	2007
I_0	370–940 MeV	LNF	Carbonara *et al.* [37]	1976
I_0	800–1100 MeV	NKS at LNS	Hirose *et al.* [38]	2009
I_0	500–4800 MeV	CEA	Crouch *et al.* [39]	1964
I_0	≈560–2560 MeV	SAPHIR at ELSA	Wu *et al.* [40]	2005
I_0	≈895–1663 MeV	CLAS at JLAB	Golovatch *et al.* [41]	2019
$I^\odot$	575–815 MeV	CB/TAPS at MAMI	Krambrich *et al.* [33]	2009
$I^\odot$	502–2350 MeV	CLAS at JLAB	Strauch *et al.* [42]	2005
$I^\odot$	1100–5400 MeV	CLAS at JLAB	Badui *et al.* [43]	2016
		$\gamma p \rightarrow p\pi^0\eta$		
I_0	≈930–2500 MeV	CB/TAPS at ELSA	Gutz *et al.* [15]	2014
I_0	≈1070–2860 MeV	CB at ELSA	Horn *et al.* [44]	2008
I_0	950–1400 MeV	CB/TAPS at MAMI	Kashevarov *et al.* [45]	2009
I_0	1000–1150 MeV	GeV-γ at LNS	Nakabayashi *et al.* [46]	2006
I_0, Σ	≈930–1500 MeV	GRAAL	Ajaka *et al.* [47]	2008
Σ	970–1650 MeV	CBELSA/TAPS at ELSA	Gutz *et al.* [48]	2008
Σ	≈1070–1550 MeV	CB/TAPS at ELSA	Gutz *et al.* [15]	2014
I^c, I^s	970–1650 MeV	CBELSA/TAPS at ELSA	Gutz *et al.* [49]	2010
I^c, I^s	≈1081–1550 MeV	CB/TAPS at ELSA	Gutz *et al.* [15]	2014
		$\gamma p \rightarrow n\pi^+\pi^0$		
I_0	300–820 MeV	TAPS at MAMI	Langgärtner *et al.* [50]	2001
I_0	≈325–800 MeV	CB/TAPS at MAMI	Zehr *et al.* [24]	2012
I_0	400–800 MeV	DAPHNE at MAMI	Braghieri *et al.* [27]	1995
I_0	400–800 MeV	DAPHNE at MAMI	Ahrens *et al.* [51]	2003
$I^\odot$	520–820 MeV	CB/TAPS at MAMI	Krambrich *et al.* [33]	2009
$I^\odot$	≈550–820 MeV	CB/TAPS at MAMI	Zehr *et al.* [24]	2012
		$\gamma n \rightarrow n\pi^0\pi^0$		
$I^\odot$	≈600–1400 MeV	CB/TAPS at MAMI	Oberle *et al.* [34]	2013
I_0, Σ	≈600–1500 MeV	GRAAL	Ajaka *et al.* [52]	2007
I_0	≈430–1371 MeV	CB/TAPS at MAMI	Dieterle *et al.* [26]	2015

TABLE IV. *(Continued.)*

Observable	Energy range E_γ^{lab}	Facility	Reference	Year of publication
		$\gamma n \rightarrow p\pi^-\pi^0$		
I_0	$\approx$370–940 MeV	LNF	Carbonara *et al.* [37]	1976
I_0	$\approx$450–800 MeV	DAPHNE at MAMI	Zabrodin *et al.* [53]	1997
I_0	$\approx$500–800 MeV	DAPHNE at MAMI	Zabrodin *et al.* [54]	1999
		$\gamma n \rightarrow n\pi^+\pi^-$		
I_0	370–940 MeV	LNF	Carbonara *et al.* [37]	1976
		$\gamma p \rightarrow pK^+K^-$		
I_0	3000–3800 MeV	CLAS at JLAB	Lombardo *et al.* [55]	2018
$I^\odot$	1100–5400 MeV	CLAS at JLAB	Badui *et al.* [43]	2016

In total, 69 sets with only one triple polarization observable have been found. All of them are shown in Table V. Hence, these are the most promising ones when it comes to the experimental verification of Moravcsik's theorem.

B. Algebraic phase-fixing method

In the following, the phase-fixing approach first developed by Nakayama in a treatment of single-meson photoproduction (i.e., for $N = 4$ amplitudes) [8] is adapted to two meson photoproduction. Thus it is possible, although tedious, to derive minimal complete sets of observables with algebraic methods.

Since the full mathematical derivation is quite extensive, all mathematical details are given in the Supplemental Material [58].

One starts by combining, i.e., adding or subtracting, the observables within one shape-class in such a way that the result only depends on two relative phases. By doing this, a "decoupled" shape-class is formed. See also Table VI.

In that way, one establishes a mathematical similarity with the shape-classes in single-meson photoproduction [8,13]. For shape-class II this would be

$$\text{IIa}: \mathcal{O}_{s1}^{II} + \mathcal{O}_{s2}^{II}, \mathcal{O}_{s3}^{II} + \mathcal{O}_{s4}^{II}, \mathcal{O}_{c1}^{II} + \mathcal{O}_{c2}^{II}, \mathcal{O}_{c3}^{II} + \mathcal{O}_{c4}^{II}, \quad (16)$$

$$\text{IIb}: \mathcal{O}_{s1}^{II} - \mathcal{O}_{s2}^{II}, \mathcal{O}_{s3}^{II} - \mathcal{O}_{s4}^{II}, \mathcal{O}_{c1}^{II} - \mathcal{O}_{c2}^{II}, \mathcal{O}_{c3}^{II} - \mathcal{O}_{c4}^{II}. \quad (17)$$

The algebraic approach shown here works out only in case the observables are selected from very particular combinations of four decoupled shape-classes.

More precisely, it has to be possible to establish a "consistency relation" [cf. Eq. 1] among the relative phases belonging to all the involved decoupled shape-classes. A necessary and sufficient condition for this can be formulated in terms of the graph constructed from the relative phases (cf. Sec. II): the latter graph has to be a cycle graph.

There exist 40 possible combinations of four decoupled shape classes fulfilling these requirements and which have the following general form:

$$\{Xa, Xb, Y, Z\}. \quad (18)$$

Two examples are shown in Fig. 3, and a complete list can be found in the Supplemental Material [58]. The following derivation holds for all combinations of shape-classes of the form given in Eq. (18).

The following discussion focuses on the example case

$$\{IIa, IIb, VIb, VIIIa\}. \quad (19)$$

For the remaining 39 cases, the derivation proceeds analogously.

For the example case (19), the consistency relation reads (cf. Table VI)

$$\underbrace{\phi_{13} + \phi_{24}}_{IIa} + \underbrace{\phi_{57} + \phi_{68}}_{IIb} = \underbrace{\phi_{18} + \phi_{27}}_{VIIIa} - \underbrace{\phi_{35} - \phi_{46}}_{VIb}. \quad (20)$$

According to Nakayama [8], the "phase-fixing" procedure starts by picking a particular combination of observables from the considered combination of shape-classes, i.e., from Eq. 19. In general, one picks two observables from shape-class Xa, two from Xb and one observable each from two different shape-classes selected from the 12 remaining. For the case at hand, these are two observables from shape-class IIa, two from IIb, one from VIb, as well as one from VIIIa. For any selection of observables which has this pattern, one has to work out the remaining discrete phase-ambiguities which exist for the associated relative phases. For each combination of possible discrete ambiguities, the consistency relation (20) then has to be evaluated. In case the consistency relations of such a combination are all linearly independent [8,13], the considered set of observables is complete.

The way forward is analogous to that done in Ref. [8]. A detailed description on how to determine all possible discrete
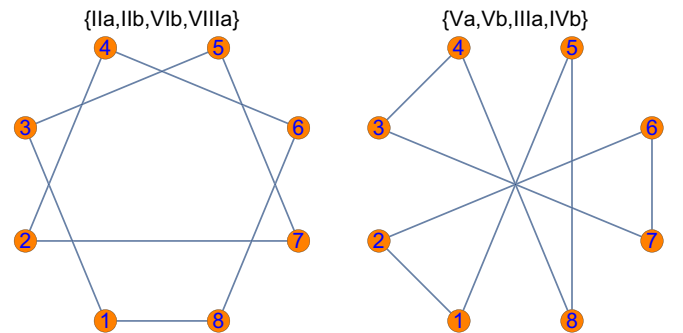

FIG. 3. Examples are shown for graph topologies which imply the possibility for a consistency relation (cf. the relative phases listed in Table VI).

TABLE V. Truly minimal sets consisting of $2N = 16$ observables with the minimal number of triple polarization observables, i.e., just $\mathcal{O}^I_4 = \mathcal{O}^{\odot}_{yy'}$. Group I observables $\{I^{\odot}, P_y, P_{y'}, \mathcal{O}^{\odot}_{yy'}, \mathcal{O}_{yy'}, P^{\odot}_{y'}, P^{\odot}_y, I_0\}$ are not explicitly shown because they are common to all complete sets. The notation used is analogous to that of Roberts and Oed [5].

(1)	P_z	$P_{x'}$	$P_{z'}$	P_x^s	P_z^c	$P_z^{\odot}$	$P_{x'}^{\odot}$	$P_{z'}^{\odot}$
(2)	P_z	P_x^s	P_z^c	$P_z^{\odot}$	$P_{x'}^c$	$P_{z'}^{\odot}$	$\mathcal{O}_{yx'}$	$\mathcal{O}_{yz'}$
(3)	P_z	P_x^s	P_z^c	$P_{x'}^{\odot}$	$P_{z'}^{\odot}$	$\mathcal{O}_{yx'}$	$\mathcal{O}_{yz'}$	$\mathcal{O}_{zy'}$
(4)	$P_{x'}$	$P_{z'}$	P_x^s	P_z^c	$P_z^{\odot}$	$P_{x'}^{\odot}$	$P_{z'}^{\odot}$	$\mathcal{O}_{zy'}$
(5)	P_x^s	P_z^c	$P_z^{\odot}$	$P_{x'}^{\odot}$	$P_{z'}^{\odot}$	$\mathcal{O}_{yx'}$	$\mathcal{O}_{yz'}$	$\mathcal{O}_{zy'}$
(6)	P_x	P_z	$P_{z'}$	P_x^s	$P_x^{\odot}$	P_z^c	$P_z^{\odot}$	$P_{z'}^{\odot}$
(7)	P_x	P_z	$P_{z'}$	P_x^s	P_z^c	$P_{z'}^{\odot}$	$\mathcal{O}_{xy'}$	$\mathcal{O}_{zy'}$
(8)	P_x	P_z	$P_{z'}$	P_x^s	P_z^c	$\mathcal{O}_{xy'}$	$\mathcal{O}_{yz'}$	$\mathcal{O}_{zy'}$
(9)	$P_{z'}$	P_x^s	$P_x^{\odot}$	P_z^c	$P_z^{\odot}$	$P_{z'}^{\odot}$	$\mathcal{O}_{xy'}$	$\mathcal{O}_{zy'}$
(10)	$P_{z'}$	P_x^s	$P_x^{\odot}$	P_z^c	$P_z^{\odot}$	$\mathcal{O}_{xy'}$	$\mathcal{O}_{yz'}$	$\mathcal{O}_{zy'}$
(11)	P_x^s	$P_x^{\odot}$	P_z^c	$P_z^{\odot}$	$P_{z'}^{\odot}$	$\mathcal{O}_{xy'}$	$\mathcal{O}_{yz'}$	$\mathcal{O}_{zy'}$
(12)	P_z	P_x^c	P_x^s	P_z^c	P_z^s	$P_z^{\odot}$	$P_{z'}^{\odot}$	$\mathcal{O}_{yz'}$
(13)	P_z	P_x^c	P_x^s	P_z^c	P_z^s	$P_{z'}^{\odot}$	$\mathcal{O}_{yz'}$	$\mathcal{O}_{zy'}$
(14)	P_x^c	P_x^s	P_z^c	P_z^s	$P_z^{\odot}$	$P_{z'}^{\odot}$	$\mathcal{O}_{yz'}$	$\mathcal{O}_{zy'}$
(15)	P_x	P_z	$P_{x'}$	P_x^s	$P_x^{\odot}$	P_z^c	$P_z^{\odot}$	$P_{x'}^{\odot}$
(16)	P_x	P_z	$P_{x'}$	P_x^s	P_z^c	$P_{x'}^{\odot}$	$\mathcal{O}_{xy'}$	$\mathcal{O}_{zy'}$
(17)	P_x	P_z	$P_{x'}$	P_x^s	P_z^c	$\mathcal{O}_{xy'}$	$\mathcal{O}_{yx'}$	$\mathcal{O}_{zy'}$
(18)	$P_{x'}$	P_x^s	$P_x^{\odot}$	P_z^c	$P_z^{\odot}$	$P_{x'}^{\odot}$	$\mathcal{O}_{xy'}$	$\mathcal{O}_{zy'}$
(19)	$P_{x'}$	P_x^s	$P_x^{\odot}$	P_z^c	$P_z^{\odot}$	$\mathcal{O}_{xy'}$	$\mathcal{O}_{yx'}$	$\mathcal{O}_{zy'}$
(20)	P_x^s	$P_x^{\odot}$	P_z^c	$P_z^{\odot}$	$P_{x'}^{\odot}$	$\mathcal{O}_{xy'}$	$\mathcal{O}_{yx'}$	$\mathcal{O}_{zy'}$
(21)	P_z	$P_{x'}$	$P_{z'}$	P_x^c	P_z^s	$P_z^{\odot}$	$P_{x'}^{\odot}$	$P_{z'}^{\odot}$
(22)	P_z	P_x^c	P_z^s	$P_z^{\odot}$	$P_{x'}^{\odot}$	$P_{z'}^{\odot}$	$\mathcal{O}_{yx'}$	$\mathcal{O}_{yz'}$
(23)	P_z	$P_{x'}$	$P_{z'}$	P_x^c	P_z^s	$\mathcal{O}_{yx'}$	$\mathcal{O}_{yz'}$	$\mathcal{O}_{zy'}$
(24)	P_z	P_x^c	P_z^s	$P_{x'}^{\odot}$	$P_{z'}^{\odot}$	$\mathcal{O}_{yx'}$	$\mathcal{O}_{yz'}$	$\mathcal{O}_{zy'}$
(25)	$P_{x'}$	$P_{z'}$	P_x^c	P_z^s	$P_z^{\odot}$	$P_{x'}^{\odot}$	$P_{z'}^{\odot}$	$\mathcal{O}_{zy'}$
(26)	P_x^c	P_z^s	$P_z^{\odot}$	$P_{x'}^{\odot}$	$P_{z'}^{\odot}$	$\mathcal{O}_{yx'}$	$\mathcal{O}_{yz'}$	$\mathcal{O}_{zy'}$
(27)	P_z	P_x^c	P_x^s	P_z^c	P_z^s	$P_z^{\odot}$	$P_{x'}^{\odot}$	$\mathcal{O}_{yx'}$
(28)	P_z	P_x^c	P_x^s	P_z^c	P_z^s	$P_{x'}^{\odot}$	$\mathcal{O}_{yx'}$	$\mathcal{O}_{zy'}$
(29)	P_x^c	P_x^s	P_z^c	P_z^s	$P_z^{\odot}$	$P_{x'}^{\odot}$	$\mathcal{O}_{yx'}$	$\mathcal{O}_{zy'}$
(30)	P_x	P_z	$P_{z'}$	P_x^c	$P_x^{\odot}$	P_z^s	$P_z^{\odot}$	$P_{z'}^{\odot}$
(31)	P_x	P_z	$P_{z'}$	P_x^c	P_z^s	$P_{z'}^{\odot}$	$\mathcal{O}_{xy'}$	$\mathcal{O}_{zy'}$
(32)	P_x	P_z	$P_{z'}$	P_x^c	P_z^s	$\mathcal{O}_{xy'}$	$\mathcal{O}_{yz'}$	$\mathcal{O}_{zy'}$
(33)	$P_{z'}$	P_x^c	$P_x^{\odot}$	P_z^s	$P_z^{\odot}$	$P_{z'}^{\odot}$	$\mathcal{O}_{xy'}$	$\mathcal{O}_{zy'}$
(34)	$P_{z'}$	P_x^c	$P_x^{\odot}$	P_z^s	$P_z^{\odot}$	$\mathcal{O}_{xy'}$	$\mathcal{O}_{yz'}$	$\mathcal{O}_{zy'}$
(35)	P_x^c	$P_x^{\odot}$	P_z^s	$P_z^{\odot}$	$P_{z'}^{\odot}$	$\mathcal{O}_{xy'}$	$\mathcal{O}_{yz'}$	$\mathcal{O}_{zy'}$
(36)	P_x	$P_{x'}$	$P_{z'}$	P_x^s	$P_x^{\odot}$	P_z^c	$P_{x'}^{\odot}$	$P_{z'}^{\odot}$
(37)	P_x	P_x^s	$P_x^{\odot}$	P_z^c	$P_z^{\odot}$	$P_{x'}^{\odot}$	$\mathcal{O}_{yx'}$	$\mathcal{O}_{yz'}$
(38)	P_x	P_x^s	P_x^c	$P_z^{\odot}$	$P_{x'}^{\odot}$	$\mathcal{O}_{xy'}$	$\mathcal{O}_{yx'}$	$\mathcal{O}_{yz'}$
(39)	$P_{x'}$	$P_{z'}$	P_x^s	$P_x^{\odot}$	P_z^c	$P_{x'}^{\odot}$	$P_{z'}^{\odot}$	$\mathcal{O}_{xy'}$
(40)	P_x^s	$P_x^{\odot}$	P_z^c	$P_z^{\odot}$	$P_{x'}^{\odot}$	$P_{z'}^{\odot}$	$\mathcal{O}_{xy'}$	$\mathcal{O}_{yz'}$
(41)	P_x	P_z	$P_{x'}$	P_x^c	$P_x^{\odot}$	P_z^s	$P_z^{\odot}$	$P_{x'}^{\odot}$
(42)	P_x	P_z	$P_{x'}$	P_x^c	P_z^s	$P_{x'}^{\odot}$	$\mathcal{O}_{xy'}$	$\mathcal{O}_{zy'}$
(43)	P_x	P_z	$P_{x'}$	P_x^c	P_z^s	$\mathcal{O}_{xy'}$	$\mathcal{O}_{yx'}$	$\mathcal{O}_{zy'}$
(44)	$P_{x'}$	P_x^c	$P_x^{\odot}$	P_z^s	$P_z^{\odot}$	$P_{x'}^{\odot}$	$\mathcal{O}_{xy'}$	$\mathcal{O}_{zy'}$
(45)	$P_{x'}$	P_x^c	$P_x^{\odot}$	P_z^s	$P_z^{\odot}$	$\mathcal{O}_{xy'}$	$\mathcal{O}_{yx'}$	$\mathcal{O}_{zy'}$
(46)	P_x^c	$P_x^{\odot}$	P_z^s	$P_z^{\odot}$	$P_{x'}^{\odot}$	$\mathcal{O}_{xy'}$	$\mathcal{O}_{yx'}$	$\mathcal{O}_{zy'}$
(47)	P_x	P_x^c	P_x^s	$P_x^{\odot}$	P_z^c	P_z^s	$P_{z'}^{\odot}$	$\mathcal{O}_{yz'}$
(48)	P_x	P_x^c	P_x^s	P_z^c	P_z^s	$P_{z'}^{\odot}$	$\mathcal{O}_{xy'}$	$\mathcal{O}_{yz'}$
(49)	P_x^c	P_x^s	$P_x^{\odot}$	P_z^c	P_z^s	$P_{z'}^{\odot}$	$\mathcal{O}_{xy'}$	$\mathcal{O}_{yz'}$
(50)	P_x	P_z	$P_x^{\odot}$	$P_z^{\odot}$	$P_{x'}^c$	$P_{z'}^s$	$\mathcal{O}_{xz'}$	$\mathcal{O}_{zx'}$
(51)	P_x	P_z	$P_{x'}^c$	$P_{z'}^s$	$\mathcal{O}_{xy'}$	$\mathcal{O}_{xz'}$	$\mathcal{O}_{zx'}$	$\mathcal{O}_{zy'}$
(52)	$P_x^{\odot}$	$P_z^{\odot}$	$P_{x'}^c$	$P_{z'}^s$	$\mathcal{O}_{xy'}$	$\mathcal{O}_{xz'}$	$\mathcal{O}_{zx'}$	$\mathcal{O}_{zy'}$
(53)	I^c	P_x	$P_x^{\odot}$	P_y^c	$\mathcal{O}_{xx'}$	$\mathcal{O}_{xz'}$	$\mathcal{O}_{zx'}$	$\mathcal{O}_{zz'}$
(54)	I^c	P_x	$P_x^{\odot}$	$P_{y'}^c$	$\mathcal{O}_{xx'}$	$\mathcal{O}_{xz'}$	$\mathcal{O}_{zx'}$	$\mathcal{O}_{zz'}$
(55)	P_x	$P_x^{\odot}$	P_y^c	$P_{y'}^c$	$\mathcal{O}_{xx'}$	$\mathcal{O}_{xz'}$	$\mathcal{O}_{zx'}$	$\mathcal{O}_{zz'}$
(56)	I^c	P_x	P_y^c	$\mathcal{O}_{xx'}$	$\mathcal{O}_{xy'}$	$\mathcal{O}_{xz'}$	$\mathcal{O}_{zx'}$	$\mathcal{O}_{zz'}$
(57)	I^c	P_x	$P_{y'}^c$	$\mathcal{O}_{xx'}$	$\mathcal{O}_{xy'}$	$\mathcal{O}_{xz'}$	$\mathcal{O}_{zx'}$	$\mathcal{O}_{zz'}$
(58)	P_x	P_y^c	$P_{y'}^c$	$\mathcal{O}_{xx'}$	$\mathcal{O}_{xy'}$	$\mathcal{O}_{xz'}$	$\mathcal{O}_{zx'}$	$\mathcal{O}_{zz'}$
(59)	I^c	$P_x^{\odot}$	P_y^c	$\mathcal{O}_{xx'}$	$\mathcal{O}_{xy'}$	$\mathcal{O}_{xz'}$	$\mathcal{O}_{zx'}$	$\mathcal{O}_{zz'}$
(60)	$P_x^{\odot}$	P_y^c	$P_{y'}^c$	$\mathcal{O}_{xx'}$	$\mathcal{O}_{xy'}$	$\mathcal{O}_{xz'}$	$\mathcal{O}_{zx'}$	$\mathcal{O}_{zz'}$
(61)	I^c	P_x	$P_x^{\odot}$	$P_{x'}^c$	$P_{x'}^s$	$P_{y'}^c$	$P_{z'}^c$	$P_{z'}^s$
(62)	P_x	$P_x^{\odot}$	P_y^c	$P_{x'}^c$	$P_{x'}^s$	$P_{y'}^c$	$P_{z'}^c$	$P_{z'}^s$
(63)	I^c	P_x	P_y^c	$P_{x'}^c$	$P_{x'}^s$	$P_{z'}^c$	$P_{z'}^s$	$\mathcal{O}_{xy'}$
(64)	I^c	$P_x^{\odot}$	P_y^c	$P_{x'}^c$	$P_{x'}^s$	$P_{z'}^c$	$P_{z'}^s$	$\mathcal{O}_{xy'}$
(65)	I^c	$P_x^{\odot}$	P_y^c	$P_{x'}^s$	$P_{y'}^c$	$P_{z'}^c$	$P_{z'}^s$	$\mathcal{O}_{xy'}$
(66)	$P_x^{\odot}$	P_y^c	$P_{x'}^c$	$P_{x'}^s$	$P_{y'}^c$	$P_{z'}^c$	$P_{z'}^s$	$\mathcal{O}_{xy'}$
(67)	I^c	I^s	P_y^c	P_y^s	$P_{x'}^c$	$P_{z'}^s$	$\mathcal{O}_{xz'}$	$\mathcal{O}_{zx'}$
(68)	I^c	I^s	$P_{x'}^c$	$P_{x'}^c$	$P_{y'}^s$	$P_{z'}^s$	$\mathcal{O}_{xz'}$	$\mathcal{O}_{zx'}$
(69)	P_y^c	P_y^s	$P_{x'}^c$	$P_{y'}^c$	$P_{y'}^s$	$P_{z'}^s$	$\mathcal{O}_{xz'}$	$\mathcal{O}_{zx'}$

TABLE V. *(Continued.)*

ambiguities and determining whether a set of consistency relations is linear independent can be found in the Supplemental Material [58].

The result for the discussed example can be found in Table VII. The results shown come only from considering the left side of Eq. 20. In general, the determination of the discrete ambiguities of the left side is easier than that of the right side. So, theoretically, even more combinations are possible. Unfortunately the discussed example (19) does not yield minimal complete sets with only one triple polarization observable. Other combination of shape classes may yield the desired result where the only triple polarization observable is contained in the diagonal shape class.

TABLE VI. The 14 decoupled shape-classes IIa, IIb, ..., VIIIa, VIIIb are listed together with their corresponding pairs of relative phases.

IIa $\longrightarrow \{\phi_{13}, \phi_{24}\}$	IIb $\longrightarrow \{\phi_{57}, \phi_{68}\}$
IIIa $\longrightarrow \{\phi_{12}, \phi_{34}\}$	IIIb $\longrightarrow \{\phi_{56}, \phi_{78}\}$
IVa $\longrightarrow \{\phi_{14}, \phi_{23}\}$	IVb $\longrightarrow \{\phi_{58}, \phi_{67}\}$
Va $\longrightarrow \{\phi_{15}, \phi_{26}\}$	Vb $\longrightarrow \{\phi_{37}, \phi_{48}\}$
VIa $\longrightarrow \{\phi_{17}, \phi_{28}\}$	VIb $\longrightarrow \{\phi_{35}, \phi_{46}\}$
VIIa $\longrightarrow \{\phi_{16}, \phi_{25}\}$	VIIb $\longrightarrow \{\phi_{38}, \phi_{47}\}$
VIIIa $\longrightarrow \{\phi_{18}, \phi_{27}\}$	VIIIb $\longrightarrow \{\phi_{36}, \phi_{45}\}$

TABLE VII. Truly minimal complete sets, consisting of $2N = 16$ observables, obtained for the example discussed in Sec. VII B. The group I observables $\{I^\odot, P_y, P_{y'}, \mathcal{O}_{yy'}^\odot, \mathcal{O}_{yy'}, P_{y'}^\odot, P_y^\odot, I_0\}$ are not explicitly shown because they are common to all complete sets. The notation used is analogous to that used by Roberts and Oed [5].

P_x	P_z	$P_x^\odot$	$P_z^\odot$	P_z^s	P_x^c	$\mathcal{O}_{zz'}^s$	$\mathcal{O}_{xz'}^c$
P_x	P_z	$P_x^\odot$	$P_z^\odot$	P_z^s	P_x^c	$\mathcal{O}_{zx'}^c$	$\mathcal{O}_{xx'}^s$
P_x	P_z	$P_x^\odot$	$P_z^\odot$	P_z^s	P_x^c	$\mathcal{O}_{zz'}^c$	$\mathcal{O}_{xz'}^s$
P_x	P_z	$P_x^\odot$	$P_z^\odot$	P_z^s	P_x^c	$\mathcal{O}_{zx'}^s$	$\mathcal{O}_{xx'}^c$
P_x	P_z	$P_x^\odot$	$P_z^\odot$	P_z^c	P_x^s	$\mathcal{O}_{zz'}^s$	$\mathcal{O}_{xz'}^c$
P_x	P_z	$P_x^\odot$	$P_z^\odot$	P_z^c	P_x^s	$\mathcal{O}_{zx'}^c$	$\mathcal{O}_{xx'}^s$
P_x	P_z	$P_x^\odot$	$P_z^\odot$	P_z^c	P_x^s	$\mathcal{O}_{zz'}^c$	$\mathcal{O}_{xz'}^s$
P_x	P_z	$P_x^\odot$	$P_z^\odot$	P_z^c	P_x^s	$\mathcal{O}_{zx'}^s$	$\mathcal{O}_{xx'}^c$
P_x	P_z	$P_x^\odot$	$P_z^\odot$	$\mathcal{O}_{zy'}^s$	$\mathcal{O}_{xy'}^c$	$\mathcal{O}_{zz'}^s$	$\mathcal{O}_{xz'}^c$
P_x	P_z	$P_x^\odot$	$P_z^\odot$	$\mathcal{O}_{zy'}^s$	$\mathcal{O}_{xy'}^c$	$\mathcal{O}_{zx'}^c$	$\mathcal{O}_{xx'}^s$
P_x	P_z	$P_x^\odot$	$P_z^\odot$	$\mathcal{O}_{zy'}^s$	$\mathcal{O}_{xy'}^c$	$\mathcal{O}_{zz'}^c$	$\mathcal{O}_{xz'}^s$
P_x	P_z	$P_x^\odot$	$P_z^\odot$	$\mathcal{O}_{zy'}^s$	$\mathcal{O}_{xy'}^c$	$\mathcal{O}_{zx'}^s$	$\mathcal{O}_{xx'}^c$
P_x	P_z	$P_x^\odot$	$P_z^\odot$	$\mathcal{O}_{zy'}^c$	$\mathcal{O}_{xy'}^s$	$\mathcal{O}_{zz'}^s$	$\mathcal{O}_{xz'}^c$
P_x	P_z	$P_x^\odot$	$P_z^\odot$	$\mathcal{O}_{zy'}^c$	$\mathcal{O}_{xy'}^s$	$\mathcal{O}_{zx'}^c$	$\mathcal{O}_{xx'}^s$
P_x	P_z	$P_x^\odot$	$P_z^\odot$	$\mathcal{O}_{zy'}^c$	$\mathcal{O}_{xy'}^s$	$\mathcal{O}_{zz'}^c$	$\mathcal{O}_{xz'}^s$
P_x	P_z	$P_x^\odot$	$P_z^\odot$	$\mathcal{O}_{zy'}^c$	$\mathcal{O}_{xy'}^s$	$\mathcal{O}_{zx'}^s$	$\mathcal{O}_{xx'}^c$
P_z^s	P_x^c	$\mathcal{O}_{xy'}$	$\mathcal{O}_{zy'}$	$\mathcal{O}_{xy'}^\odot$	$\mathcal{O}_{zy'}^\odot$	$\mathcal{O}_{zz'}^s$	$\mathcal{O}_{xz'}^c$
P_z^s	P_x^c	$\mathcal{O}_{xy'}$	$\mathcal{O}_{zy'}$	$\mathcal{O}_{xy'}^\odot$	$\mathcal{O}_{zy'}^\odot$	$\mathcal{O}_{zx'}^c$	$\mathcal{O}_{xx'}^s$
P_z^s	P_x^c	$\mathcal{O}_{xy'}$	$\mathcal{O}_{zy'}$	$\mathcal{O}_{xy'}^\odot$	$\mathcal{O}_{zy'}^\odot$	$\mathcal{O}_{zz'}^c$	$\mathcal{O}_{xz'}^s$
P_z^s	P_x^c	$\mathcal{O}_{xy'}$	$\mathcal{O}_{zy'}$	$\mathcal{O}_{xy'}^\odot$	$\mathcal{O}_{zy'}^\odot$	$\mathcal{O}_{zx'}^s$	$\mathcal{O}_{xx'}^c$
P_z^c	P_x^s	$\mathcal{O}_{xy'}$	$\mathcal{O}_{zy'}$	$\mathcal{O}_{xy'}^\odot$	$\mathcal{O}_{zy'}^\odot$	$\mathcal{O}_{zz'}^s$	$\mathcal{O}_{xz'}^c$
P_z^c	P_x^s	$\mathcal{O}_{xy'}$	$\mathcal{O}_{zy'}$	$\mathcal{O}_{xy'}^\odot$	$\mathcal{O}_{zy'}^\odot$	$\mathcal{O}_{zx'}^c$	$\mathcal{O}_{xx'}^s$
P_z^c	P_x^s	$\mathcal{O}_{xy'}$	$\mathcal{O}_{zy'}$	$\mathcal{O}_{xy'}^\odot$	$\mathcal{O}_{zy'}^\odot$	$\mathcal{O}_{zz'}^c$	$\mathcal{O}_{xz'}^s$
P_z^c	P_x^s	$\mathcal{O}_{xy'}$	$\mathcal{O}_{zy'}$	$\mathcal{O}_{xy'}^\odot$	$\mathcal{O}_{zy'}^\odot$	$\mathcal{O}_{zx'}^s$	$\mathcal{O}_{xx'}^c$
$\mathcal{O}_{xy'}$	$\mathcal{O}_{zy'}$	$\mathcal{O}_{xy'}^\odot$	$\mathcal{O}_{zy'}^\odot$	$\mathcal{O}_{zy'}^s$	$\mathcal{O}_{xy'}^c$	$\mathcal{O}_{zz'}^s$	$\mathcal{O}_{xz'}^c$
$\mathcal{O}_{xy'}$	$\mathcal{O}_{zy'}$	$\mathcal{O}_{xy'}^\odot$	$\mathcal{O}_{zy'}^\odot$	$\mathcal{O}_{zy'}^s$	$\mathcal{O}_{xy'}^c$	$\mathcal{O}_{zx'}^c$	$\mathcal{O}_{xx'}^s$
$\mathcal{O}_{xy'}$	$\mathcal{O}_{zy'}$	$\mathcal{O}_{xy'}^\odot$	$\mathcal{O}_{zy'}^\odot$	$\mathcal{O}_{zy'}^s$	$\mathcal{O}_{xy'}^c$	$\mathcal{O}_{zz'}^c$	$\mathcal{O}_{xz'}^s$
$\mathcal{O}_{xy'}$	$\mathcal{O}_{zy'}$	$\mathcal{O}_{xy'}^\odot$	$\mathcal{O}_{zy'}^\odot$	$\mathcal{O}_{zy'}^s$	$\mathcal{O}_{xy'}^c$	$\mathcal{O}_{zx'}^s$	$\mathcal{O}_{xx'}^c$
$\mathcal{O}_{xy'}$	$\mathcal{O}_{zy'}$	$\mathcal{O}_{xy'}^\odot$	$\mathcal{O}_{zy'}^\odot$	$\mathcal{O}_{zy'}^c$	$\mathcal{O}_{xy'}^s$	$\mathcal{O}_{zz'}^s$	$\mathcal{O}_{xz'}^c$
$\mathcal{O}_{xy'}$	$\mathcal{O}_{zy'}$	$\mathcal{O}_{xy'}^\odot$	$\mathcal{O}_{zy'}^\odot$	$\mathcal{O}_{zy'}^c$	$\mathcal{O}_{xy'}^s$	$\mathcal{O}_{zx'}^c$	$\mathcal{O}_{xx'}^s$
$\mathcal{O}_{xy'}$	$\mathcal{O}_{zy'}$	$\mathcal{O}_{xy'}^\odot$	$\mathcal{O}_{zy'}^\odot$	$\mathcal{O}_{zy'}^c$	$\mathcal{O}_{xy'}^s$	$\mathcal{O}_{zz'}^c$	$\mathcal{O}_{xz'}^s$
$\mathcal{O}_{xy'}$	$\mathcal{O}_{zy'}$	$\mathcal{O}_{xy'}^\odot$	$\mathcal{O}_{zy'}^\odot$	$\mathcal{O}_{zy'}^c$	$\mathcal{O}_{xy'}^s$	$\mathcal{O}_{zx'}^s$	$\mathcal{O}_{xx'}^c$

VIII. IMPLICATIONS FOR EXPERIMENTALISTS

The experimental verification of complete sets, in the framework of single pseudoscalar meson photoproduction, was studied, for example, by Ireland [9] and Vrancx *et al.* [59]. They concluded that, as soon as the data have a finite measurement uncertainty, it might not be possible to determine unique solutions for the amplitudes in case one uses a mathematical, minimal complete set of observables. It is believed that additional observables could resolve the ambiguity. Thus it is important to measure more than 16 observables [9].

Observables which are relatively easy to measure rank in the categories $\mathcal{B}$, $\mathcal{T}$, $\mathcal{BT}$ because they do not require a recoil polarimeter. Even though they form a group of 16 observables, they do not form a complete set, which was verified numerically in this study. The measurement of some well-chosen observables from the categories $\mathcal{R}$, $\mathcal{BR}$, $\mathcal{TR}$, and $\mathcal{BTR}$ is essential. Out of the 69 possible complete sets that require the measurement of only one triple polarization observable and which are listed in Table V, the sets (6), (12), (15), (27), (30), (41), and (47) contain the minimal number of recoil polarization observables, e.g., the set (15) contains the following observables:

$$
\begin{aligned}
&\{I^\odot, P_y, P_{y'}, \mathcal{O}_{yy'}^\odot, \mathcal{O}_{yy'}, P_{y'}^\odot, P_y^\odot, I_0, P_x, P_z, P_{x'}, P_x^s, \\
&P_x^\odot, P_z^c, P_z^\odot, P_{x'}^\odot\}.
\end{aligned} \tag{21}
$$

Data exist for eight of these observables $[I_0, I^\odot, P_x, P_y, P_{y'}, \mathcal{O}_{yy'}(= -I^c), P_x^s, P_z^\odot]$ for the $p\pi^0\pi^0$ final state, albeit not having a perfect overlap of the energy and angular ranges covered by the different data sets (see Table IV). The remaining eight observables could be measured in the future in three different experiments using a linearly polarized photon beam with a longitudinally polarized target (P_z, P_z^c), using a circularly polarized photon beam and a transversely polarized target ($P_x^\odot$, $P_y^\odot$), and by employing a recoil polarimeter in addition to the latter configuration, the observables $P_{x'}$, $P_{x'}^\odot$, $P_{y'}^\odot$, and $\mathcal{O}_{yy'}^\odot$ can be obtained as well.

IX. CONCLUSION AND OUTLOOK

Within this paper, the problem of finding complete sets for two pseudoscalar meson photoproduction was studied. For this purpose, a slightly modified version of Moravcsik's theorem was applied. This method is capable of extracting complete sets of observables in a totally automated manner. The automation capability, easy accessibility, as well as the adaptability for reactions with arbitrary N are the strengths of Moravcsik's theorem. However, it turns out that the resulting sets from Moravcsik are slightly overcomplete since each observable depends on more than one bilinear product. For this reason, a numerical- as well as an algebraic method are discussed in order to reduce these sets to minimal complete sets containing $2N = 16$ observables. The characteristics of the minimal sets are discussed. Finally, 69 minimal complete sets containing the minimal number of triple polarization observables, namely only one, are presented. From these subsets in combination with the extensive overview of already performed measurements in two pseudoscalar meson photoproduction, the most promising set of observables, which could be measured in the near future, is presented.

Further studies could be performed on how Moravcsik's theorem should be adapted in order to yield directly minimal complete sets. This would decrease the numerical effort enormously and would make the theorem even more accessible.

APPENDIX: ALGORITHM TO CHECK FOR COMPLETENESS

The following algorithm was designed by Tiator [60] and was already applied in Ref. [61]. It is used to check if a set of observables is able to resolve continuous as well as discrete ambiguities. The starting point is a system of multivariate homogeneous polynomials $f_1(\vec{t}), \dots, f_n(\vec{t})$. The input is a vector of N complex amplitudes t_i. Without loss of generality, the overall phase of the complex amplitudes is fixed by requiring $\mathrm{Re}(t_1) > 0$ and $\mathrm{Im}(t_1) = 0$. In a next step an N-dimensional solution vector $\vec{s}$ is formed. It consist of $2N - 1$ randomly chosen prime numbers within a certain range. These

serve as values for the real and imaginary parts of t_i. Using prime numbers and increasing the range from which they are chosen should reduce the chance to land on a singularity in the solution space, where the "condition of equal magnitudes of relative phases" [8] is met.

Finally, the polynomial system

$$
\begin{aligned}
f_1(\vec{t}) &= g_1, \\
&\vdots \\
f_n(\vec{t}) &= g_n,
\end{aligned}
\tag{A1}
$$

is constructed, where $g_i = f_i(\vec{s})$ is a scalar quantity. The function *NSolve* from *Mathematica* [56] is employed to solve the algebraic system for the variables $t_1, \dots, t_N$. According to the Wolfram *Mathematica* documentation [62,63]: "For systems of algebraic equations, NSolve computes a numerical Gröbner basis using an efficient monomial ordering, then uses eigensystem methods to extract numerical roots."

The system of polynomials is said to be complete if only one solution is found which furthermore is equivalent to $\vec{s}$.

[1] V. Sokhoyan *et al.*, High-statistics study of the reaction $\gamma p \to p2\pi^0$, Eur. Phys. J. A **51**, 95 (2015).

[2] A. Fix and H. Arenhövel, Double-pion photoproduction on nucleon and deuteron, Eur. Phys. J. A **25**, 115 (2005).

[3] C. G. Fasano, F. Tabakin, and B. Saghai, Spin observables at threshold for meson photoproduction, Phys. Rev. C **46**, 2430 (1992).

[4] G. Knöchlein, D. Drechsel, and L. Tiator, Photo- and electroproduction of eta mesons, Z. Phys. A: Hadrons Nucl. **352**, 327 (1995).

[5] W. Roberts and T. Oed, Polarization observables for two-pion production off the nucleon, Phys. Rev. C **71**, 055201 (2005).

[6] W.-T. Chiang and F. Tabakin, Completeness rules for spin observables in pseudoscalar meson photoproduction, Phys. Rev. C **55**, 2054 (1997).

[7] I. Barker, A. Donnachie, and J. Storrow, Complete experiments in pseudoscalar photoproduction, Nucl. Phys. B **95**, 347 (1975).

[8] K. Nakayama, Explicit derivation of the completeness condition in pseudoscalar meson photoproduction, Phys. Rev. C **100**, 035208 (2019).

[9] D. G. Ireland, Information content of polarization measurements, Phys. Rev. C **82**, 025204 (2010).

[10] G. Chew, M. Goldberger, F. Low, and Y. Nambu, Relativistic dispersion relation approach to photomeson production, Phys. Rev. **106**, 1345 (1957).

[11] H. Arenhövel and A. Fix, Complete set of observables for photoproduction of two pseudoscalars on a nucleon, Phys. Rev. C **89**, 034003 (2014).

[12] M. J. Moravcsik, Resolving the discrete ambiguities in amplitude determinations, J. Math. Phys. **26**, 211 (1985).

[13] Y. Wunderlich, P. Kroenert, F. Afzal, and A. Thiel, Moravcsik's theorem on complete sets of polarization observables reexamined, Phys. Rev. C **102**, 034605 (2020).

[14] T. Seifen *et al.*, Measurement of polarization observables in neutral double pion photoproduction off the proton with the CBELSA/TAPS experiment, EPJ Web Conf. **241**, 01016 (2020).

[15] E. Gutz, V. Crede, V. Sokhoyan, H. van Pee, A. Anisovich, J. Bacelar, B. Bantes, O. Bartholomy, D. Bayadilov, R. Beck *et al.*, High statistics study of the reaction $\gamma p \to p\pi^0\eta$, Eur. Phys. J. A **50**, 74 (2014).

[16] W. Briscoe, M. Doering, H. Haberzettl, I. Strakovsky, and R. Workman, Said database, http://gwdac.phys.gwu.edu, accessed 16 July 2020.

[17] D. G. Ireland, E. Pasyuk, and I. Strakovsky, Photoproduction reactions and non-strange baryon spectroscopy, Prog. Part. Nucl. Phys. **111**, 103752 (2020).

[18] M. Sikora, D. Glazier, and D. Watts, Recoil polarimetry in meson photoproduction at MAMI, Chin. Phys. C **33**, 1373 (2009).

[19] K.-T. Brinkmann, Recoil polarization measurements, EPJ Web Conf. **134**, 03007 (2017).

[20] F. Härter, J. Ahrens, R. Beck, B. Krusche, V. Metag, M. Schmitz, H. Ströher, T. Walcher, and M. Wolf, Two neutral pion photoproduction off the proton between threshold and 800 MeV, Phys. Lett. B **401**, 229 (1997).

[21] M. Wolf, J. Ahrens, R. Beck, V. Hejny, J. Kellie, M. Kotulla, B. Krusche, V. Kuhr, R. Leukel, V. Metag *et al.*, Photoproduction of neutral pion pairs from the proton, Eur. Phys. J. A **9**, 5 (2000).

[22] V. Kleber, P. Achenbach, J. Ahrens, R. Beck, V. Hejny, J. Kellie, M. Kotulla, B. Krusche, V. Kuhr, R. Leukel *et al.*, Double-π^0 photoproduction from the deuteron, Eur. Phys. J. A **9**, 1 (2000).

[23] M. Kotulla, J. Ahrens, J. Annand, R. Beck, D. Hornidge, S. Janssen, B. Krusche, J. McGeorge, I. MacGregor, J. Messchendorp *et al.*, Double π^0 photoproduction off the proton at threshold, Phys. Lett. B **578**, 63 (2004).

[24] F. Zehr, B. Krusche, P. Aguar, J. Ahrens, J. Annand, H. Arends, R. Beck, V. Bekrenev, A. Boillat, A. Braghieri *et al.*, Photoproduction of $\pi^0\pi^0$- and $\pi^0\pi^+$-pairs off the proton from threshold to the second resonance region, Eur. Phys. J. A **48**, 98 (2012).

[25] V. Kashevarov, A. Fix, S. Prakhov, P. Aguar-Bartolome, J. Annand, H. Arends, K. Bantawa, R. Beck, V. Bekrenev, H. Berghäuser *et al.*, Experimental study of the $\gamma p \to \pi^0\pi^0 p$ reaction with the Crystal Ball/TAPS detector system at the Mainz microtron, Phys. Rev. C **85**, 064610 (2012).

[26] M. Dieterle, M. Oberle, J. Ahrens, J. Annand, H. Arends, K. Bantawa, P. Bartolome, R. Beck, V. Bekrenev, H. Berghäuser *et al.*, Photoproduction of π^0-pairs off protons and off neutrons, Eur. Phys. J. A **51**, 142 (2015).

[27] A. Braghieri, L. Murphy, J. Ahrens, G. Audit, N. d'Hose, V. Isbert, S. Kerhoas, M. Mac Cormick, P. Pedroni, T. Pinelli *et al.*, Total cross section measurement for the three double pion photoproduction channels on the proton, Phys. Lett. B **363**, 46 (1995).

[28] J. Ahrens, S. Altieri, J. Annand, G. Anton, H.-J. Arends, K. Aulenbacher, R. Beck, C. Bradtke, A. Braghieri, N. Degrande *et al.*, Intermediate resonance excitation in the $\gamma p \to p\pi^0\pi^0$ reaction, Phys. Lett. B **624**, 173 (2005).

[29] A. Sarantsev, M. Fuchs, M. Kotulla, U. Thoma, J. Ahrens, J. Annand, A. Anisovich, G. Anton, R. Bantes, O. Bartholomy *et al.*, New results on the Roper resonance and the P11 partial wave, Phys. Lett. B **659**, 94 (2008).

[30] U. Thoma, M. Fuchs, A. Anisovich, G. Anton, R. Bantes, O. Bartholomy, R. Beck, Y. Beloglazov, V. Crede, A. Ehmanns *et al.*, N^* and Δ^* decays into $N\pi^0\pi^0$, Phys. Lett. B **659**, 87 (2008).

[31] A. Thiel, V. Sokhoyan, E. Gutz, H. van Pee, A. Anisovich, J. Bacelar, B. Bantes, O. Bartholomy, D. Bayadilov, R. Beck *et al.*, Three-Body Nature of $N*$ and $\Delta*$ Resonances from Sequential Decay Chains, Phys. Rev. Lett. **114**, 091803 (2015).

[32] Y. Assafiri, O. Bartalini, V. Bellini, J. P. Bocquet, S. Bouchigny, M. Capogni, M. Castoldi, A. D'Angelo, J. Didelez, R. Di Salvo *et al.*, Double π^0 Photoproduction on the Proton at GRAAL, Phys. Rev. Lett. **90**, 222001 (2003).

[33] D. Krambrich, F. Zehr, A. Fix, L. Roca, P. Aguar, J. Ahrens, J. Annand, H. Arends, R. Beck, V. Bekrenev *et al.*, Beam-Helicity Asymmetries in Double-Pion Photoproduction off the Proton, Phys. Rev. Lett. **103**, 052002 (2009).

[34] M. Oberle, B. Krusche, J. Ahrens, J. Annand, H. Arends, K. Bantawa, P. Bartolome, R. Beck, V. Bekrenev, H. Berghäuser *et al.*, Measurement of the beam-helicity asymmetry $I^{\odot}$ in the photoproduction of π^0-pairs off the proton and off the neutron, Phys. Lett. B **721**, 237 (2013).

[35] M. Dieterle, L. Witthauer, A. Fix, S. Abt, P. Achenbach, P. Adlarson, F. Afzal, P. A. Bartolome, Z. Ahmed, J. R. M. Annand *et al.*, Helicity-Dependent Cross Sections for the Photoproduction of π^0 Pairs from Nucleons, Phys. Rev. Lett. **125**, 062001 (2020).

[36] J. Ahrens, S. Altieri, J. Annand, H.-J. Arends, R. Beck, M. Blackston, C. Bradtke, A. Braghieri, N. d'Hose, H. Dutz *et al.*, First measurement of the helicity dependence for the $\gamma p \to p\pi$ reaction, Eur. Phys. J. A **34**, 11 (2007).

[37] F. Carbonara, G. Chiefari, E. Drago, G. Gialanella, L. Merola, M. Napolitano, R. Rinzivillo, G. Sciacca, V. Rossi, and G. Susinno, Analysis of $\gamma n \to n\pi^+\pi^-$ and $\gamma n \to p\pi^-\pi^0$ reactions from threshold up to 1 GeV, Nuovo Cimento A **36**, 219 (1976).

[38] K. Hirose, M. Ejima, T. Fujibayashi, Y. Fujii, K. Futatsukawa, O. Hashimoto, T. Ishikawa, S. Kameoka, H. Kanda, F. Kato *et al.*, Study of double pion photoproduction on the deuteron, Phys. Lett. B **674**, 17 (2009).

[39] H. Crouch, Jr., R. Hargraves, B. Kendall, R. Lanou, A. Shapiro, M. Widgoff, G. Fischer, A. Brenner, M. Law, E. Ronat *et al.*, Gamma-Ray Proton Interactions between 0.5 and 4.8 BeV, Phys. Rev. Lett. **13**, 636 (1964).

[40] C. Wu, J. Barth, W. Braun, J. Ernst, K.-H. Glander, J. Hannappel, N. Jöpen, H. Kalinowsky, F. Klein, F. Klein *et al.*, Photoproduction of ρ mesons and δ-baryons in the reaction $\gamma p \to p\pi^+\pi^-$ at energies up to $\sqrt{s} = 2.6$ GeV, Eur. Phys. J. A **23**, 317 (2005).

[41] E. Golovatch *et al.*, First results on nucleon resonance photo-couplings from the $\gamma p \to \pi^+\pi^- p$ reaction, Phys. Lett. B **788**, 371 (2019).

[42] S. Strauch, B. Berman, G. Adams, P. Ambrozewicz, M. Anghinolfi, B. Asavapibhop, G. Asryan, G. Audit, H. Avakian, H. Bagdasaryan *et al.*, Beam-Helicity Asymmetries in Double-Charged-Pion Photoproduction on the Proton, Phys. Rev. Lett. **95**, 162003 (2005).

[43] R. Badui, J. Bono, L. Guo, and B. A. Raue, The beam-helicity asymmetry for $\gamma p \to pK^+K^-$ and $\gamma p \to p\pi^+\pi^-$, AIP Conf. Proc. **1735**, 040014 (2016).

[44] I. Horn, A. Anisovich, G. Anton, R. Bantes, O. Bartholomy, R. Beck, Y. Beloglazov, R. Bogendörfer, R. Castelijns, V. Crede *et al.*, Evidence for a Parity Doublet Δ (1920) P33 and Δ (1940) D33 from $\gamma p \to p\pi^0\eta$, Phys. Rev. Lett. **101**, 202002 (2008).

[45] V. Kashevarov, A. Fix, P. Aguar-Bartolomé, L. Akasoy, J. Annand, H. Arends, K. Bantawa, R. Beck, V. Bekrenev, H. Berghäuser *et al.*, Photoproduction of $\pi^0\eta$ on protons and the $\Delta(1700)$ D_{33}-resonance, Eur. Phys. J. A **42**, 141 (2009).

[46] T. Nakabayashi, H. Fukasawa, R. Hashimoto, T. Ishikawa, T. Iwata, H. Kanda, J. Kasagi, T. Kinoshita, K. Maeda, F. Miyahara *et al.*, Photoproduction of η mesons off protons for $E_\gamma \leqslant 1.15$ GeV, Phys. Rev. C **74**, 035202 (2006).

[47] J. Ajaka, Y. Assafiri, O. Bartalini, V. Bellini, S. Bouchigny, M. Castoldi, A. D'Angelo, J. Didelez, R. Di Salvo, M. Döring *et al.*, Simultaneous Photoproduction of η and π^0 Mesons on the Proton, Phys. Rev. Lett. **100**, 052003 (2008).

[48] E. Gutz, V. Sokhoyan, H. van Pee, A. Anisovich, J. Bacelar, B. Bantes, O. Bartholomy, D. Bayadilov, R. Beck, Y. Beloglazov *et al.*, Measurement of the beam asymmetry Σ in $\pi^0\eta$ production off the proton with the CBELSA/TAPS experiment, in *NSTAR 2007*, edited by H. W. Hammer, V. Kleber, U. Thoma, and H. Schmieden (Springer, Berlin, Heidelberg, 2008), pp. 190–192.

[49] E. Gutz, V. Sokhoyan, H. van Pee, A. Anisovich, J. Bacelar, B. Bantes, O. Bartholomy, D. Bayadilov, R. Beck, Y. Beloglazov *et al.*, Photoproduction of meson pairs: First measurement of the polarization observable Is, Phys. Lett. B **687**, 11 (2010).

[50] W. Langgärtner, J. Ahrens, R. Beck, V. Hejny, M. Kotulla, B. Krusche, V. Kuhr, R. Leukel, J. D. McGregor, J. G. Messchendorp *et al.*, Direct Observation of a ρ Decay of the $D_{13}(1520)$ Baryon Resonance, Phys. Rev. Lett. **87**, 052001 (2001).

[51] J. Ahrens, S. Altieri, J. Annand, G. Anton, H.-J. Arends, K. Aulenbacher, R. Beck, C. Bradtke, A. Braghieri, N. Degrande *et al.*, Helicity dependence of the $\gamma p \to n\pi^+\pi^0$ reaction in the second resonance region, Phys. Lett. B **551**, 49 (2003).

[52] J. Ajaka, Y. Assafiri, O. Bartalini, V. Bellini, S. Bouchigny, M. Castoldi, A. d'Angelo, J. Didelez, R. Di Salvo, A. Fantini *et al.*, Double π^0 photoproduction on the neutron at GRAAL, Phys. Lett. B **651**, 108 (2007).

[53] A. Zabrodin, G. Audit, R. Beck, A. Braghieri, N. D'Hose, B. Dolbilkin, S. J. Hall, V. Isbert, L. Y. Murphy, P. Pedroni *et al.*, Total cross section measurement of the $\gamma n \to p\pi^-\pi^0$ reaction, Phys. Rev. C **55**, R1617(R) (1997).

[54] A. Zabrodin, G. Audit, R. Beck, A. Braghieri, N. D'Hose, S. J. Hall, J. D. Kellie, M. MacCormick, L. Y. Murphy, A. Panzeri *et al.*, Invariant mass distributions of the $\gamma n \rightarrow p\pi^-\pi^0$ reaction, Phys. Rev. C **60**, 055201 (1999).

[55] S. Lombardo *et al.* (CLAS Collaboration), Photoproduction of K^+K^- meson pairs on the proton, Phys. Rev. D **98**, 052009 (2018).

[56] Wolfram, Inc., Mathematica, Version 12.1 (Champaign, 2020).

[57] J. Bezanson, A. Edelman, S. Karpinski, and V. B. Shah, JULIA: A fresh approach to numerical computing, SIAM Rev. **59**, 65 (2017).

[58] See Supplemental Material at http://link.aps.org/supplemental/10.1103/PhysRevC.103.014607 for a demonstration of the algebraic reduction of overcomplete sets.

[59] T. Vrancx, J. Ryckebusch, T. Van Cuyck, and P. Vancraeyveld, Incompleteness of complete pseudoscalar-meson photoproduction, Phys. Rev. C **87**, 055205 (2013).

[60] L. Tiator (private communication).

[61] L. Tiator, R. L. Workman, Y. Wunderlich, and H. Haberzettl, Amplitude reconstruction from complete electroproduction experiments and truncated partial-wave expansions, Phys. Rev. C **96**, 025210 (2017).

[62] Some notes on internal implementation, https://reference.wolfram.com/language/tutorial/SomeNotesOnInternalImplementation.html, accessed 25 May 2020.

[63] I. N. Bronstein and K. A. Semendjajew, in *Taschenbuch der Mathematik*, 19th ed., edited by G. Grosche and V. Ziegler (BSB B. G. Teubner Verlagsgesellschaft, Nauka-Verlag, Leipzig, Moskau, 1979).